THE CRYOTRON AS A LINEAR AMPLIFIER

by

Dieter K. Schroder

A thesis submitted to the
Faculty of Graduate Studies and Research
in partial fulfillment of the requirements
for the degree of
Master of Engineering

Department of Electrical Engineering
McGill University
Montreal

August 1964

Abstract

The possibility of using a wire-wound cryotron as an amplifier is examined and it is shown that current and voltage gains greater than unity are possible. Advantages of a superconducting ground plane are investigated and it is subsequently used in all experimental work. The frequency response of the device is determined by the time constants of the control circuit and load impedance, resulting in an upper frequency limit of approximately 10 Kc/s. Barkhausen noise is the dominant noise, due to discontinuous movements of superconducting and normal domains in the intermediate state of the gate. The difficulty of nucleating superconducting domains in a resistive surrounding is believed responsible for hysteresis when the dominant magnetic field is the self-field of the gate. Under certain experimental conditions fluctuations of the gate resistance are observed, and are shown to be due to thermal instabilities.

Acknowledgements

The author wishes to express his sincere gratitude to Dr. G.W. Farnell for his guidance throughout this research project. He also expresses his appreciation to the staff of the Department of Electrical Engineering for aid and suggestions in the course of this work.

The financial assistance by the National Research Council in the form of two summer supplements and support of the entire project through a research grant is gratefully acknowledged, as is the award of the Northern Electric Fellowship 1963-1964.

Finally, the author wishes to thank his wife for typing the thesis.

Table of Contents

1. Introduction

The wire-wound cryotron was discovered in 1954, although its principle of operation had been utilized before that time. The first application was as a switching element and since then many improvements have been made, notably that of the development of the thin-film cryotron. But almost all research has been directed towards the application of this device as a computer switching element with a superconducting computer as a goal.

The possibility of using the cryotron as an amplifier has received little attention, and it is this application that is studied in this work for the wire-wound cryotron. The principle of operation and the basic characteristics are discussed and the experimental techniques are presented. Models are derived for low- and high-frequency operation and they are used to theoretically predict the frequency response. Experimental results show that the frequency response has an upper limit of approximately 10 Kc/s. Because of the low resistances encountered at the low temperatures of operation of the device, normally negligible inductances become extremely important and in effect determine the upper limit.

Factors that need be considered in the design of a wire-wound cryotron are examined, and it is shown that high-power devices can be built.

Superconducting hysteresis is a phenomenon that occurs as a result of the bistable property of a superconductor in the intermediate state. In this state the superconductor consists of a number of normal and superconducting domains and for the same currents and magnetic fields two different domain configurations are possible. This is dependent upon whether the superconductor is in the intermediate state as a result of a normal-to-superconducting

or a superconducting-to-normal transition. It is discussed why hysteresis is not always observed and it is shown that when it does occur, it has a discontinuous,steplike resistance transition between the superconducting and and the normal state associated with it. These discontinuous jumps in resistance are a result of sudden domain motion and are the source of Barkhausen noise.

Since hysteresis does not exist for all transitions, there is then an optimum region of operation for the cryotron used as an amplifier.

There are two major parts to the thesis. One deals with models that represent the cryotron at different frequencies and with theoretical and experimental gain- and frequency response curves. The other is concerned with the internal mechanism in the superconductor that gives rise to such phenomena as hysteresis and noise.

2. Basic Characteristics

The principle of operation of a cryotron rests on the property of a superconductor that allows the superconductive state to be quenched by a magnetic field, that is, resistance can be restored in a superconductive material by the application of a magnetic field. The field necessary to restore the first trace of resistance is in this work defined as H_c, the critical magnetic field. An approximate parabolic relationship between H_c and the temperature of a superconductor is shown in Fig.1 and can be expressed by the equation

$$H_c = H_o(1 - (T/T_c)^2) \qquad (1)$$

where H_o is the critical magnetic field at absolute zero temperature and T_c is the transition temperature below which the resistance of the material has an immeasurably small value.

The cryotron is operated at constant temperature in a varying magnetic field, corresponding to the line between points A and B in Fig.1.

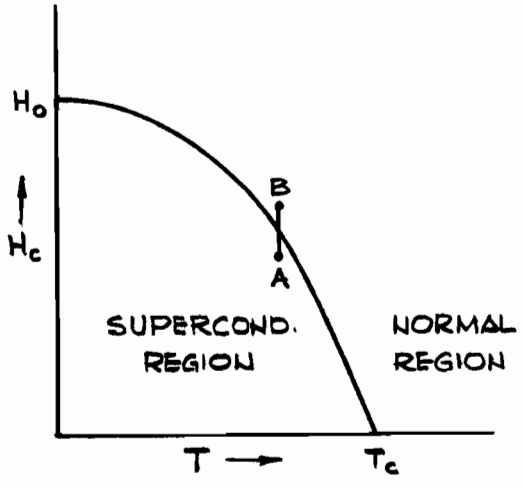

Fig. 1
The Critical Magnetic Field as a Function of Temperature

Templeton(1) employed the principle of changing the state of a piece of wire from the superconductive to the normal state to build a superconductive reversing switch. A tantalum wire was switched between the two states by a controlled magnetic field and the device found an application in the measurement of low thermal voltages. To obtain more sensitive measurements, he then devised a superconducting modulator(2) in which a tantalum wire was switched between the two stable states by an audio-frequency alternating magnetic field. The modulated wire was connected in series with the low emf that was to be measured and the primary of a miniature transformer. The small static voltage was chopped and the resulting a-c signal transformed to a higher voltage to be measured with conventional equipment.

De Vroomen and Van Baarle(3) built a chopper amplifier on a similar basis. It could measure voltages of 10^{-11} volts and was somewhat more refined than Templeton's in that more emphasis was placed on the elimination of magnetic pick-up voltages, which were as high as 10^{-6} volts.

At the 1960 Solid State Circuits Conference, Templeton(4) presented a paper describing a modified version of the superconductive reversing switch. Whereas in the original switch the superconductive element was either on or off, that is, in the S or N-state*, in the modified version it was held at some point in the transition region (see Fig.3). A control winding surrounding each element could then move the operating point along the transition curve and the change in the output was detected by a galvanometer resulting in a superconductive bridge amplifier.

It was the late Dudley Buck(5), however, who investigated the relationship between the current in a straight S-wire and the current in an S-coil wound around it. His device consisted of a tantalum wire called the gate, around which

* S and N represent 'superconductive' and 'normal', respectively.

was wound a finer wire called the control, as shown in Fig.2. The gate wire had a low H_c while the control was a high H_c material. By adjusting the control current the gate could be switched from the S to the N-state and vice versa.

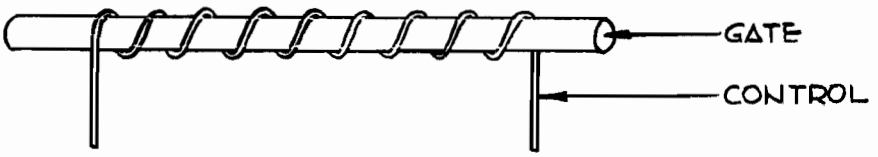

Fig. 2
Wire-Wound Cryotron

In 1954 Buck coined the word 'cryotron' which now is defined by The IRE Standards on Superconductive Terms (6) as follows:

> A superconductive device in which current in one or more input circuits magnetically controls the superconducting-to-normal transition in one or more output circuits, provided the current in each output circuit is less than its critical value.

In each of the above-mentioned devices, the principle of the cryotron was used in a switching application, that is, a wire was switched between the S and N-states corresponding to operation at point A and to the left of it or B and to the right of it in Fig.3.

This figure also shows that the transition from A to B is not a discontinuous one, rather the resistance of the specimen is gradually increased from zero to its normal value. If the gate of the cryotron is biased at point C, then small changes in the control current result in changes in

the magnetic field, which in turn shift point C along the curve. Physically it changes the resistance of the gate and thus the gate current, so that in effect the control current controls the gate current, provided the gate is held at its proper operating point.

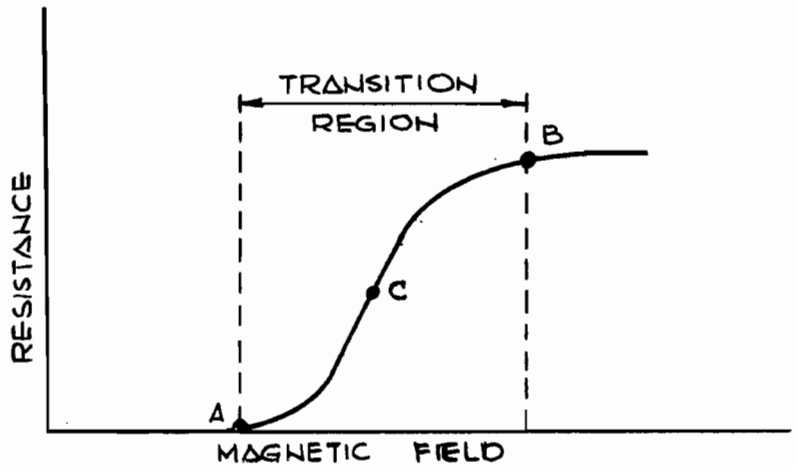

Fig. 3
Resistance as a Function of a Magnetic Field
for a Superconductor

This can be understood more easily by examining two sets of curves, called the 'Characteristic Curves' and defined as those showing the gate current plotted against gate voltage with control current as the running parameter (Fig.4), and the 'Voltage Transition Curves', defined as those showing the gate voltage against the control current with the gate current as the running parameter (Fig.5). Other curves, such as the 'Resistance Transition' and the 'Current Transfer Curves' can be derived from these two basic ones.

The control current generates a longitudinal magnetic field and the gate current produces a circular field that is perpendicular to the gate axis at any point on the surface of the wire. The resultant field at any point of the gate is thus the vector sum of the control and gate fields which are mutually perpendicular.

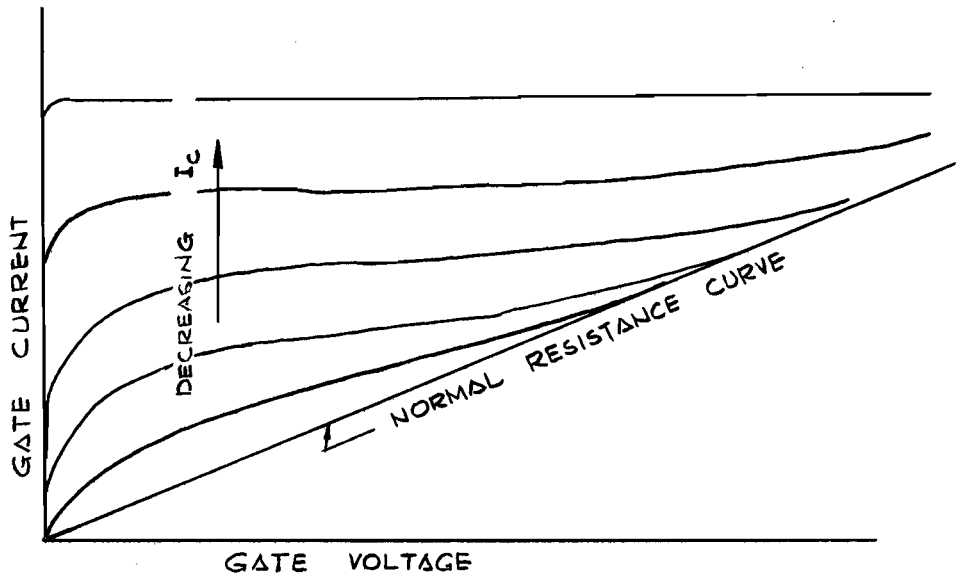

Fig. 4

Characteristic Curves

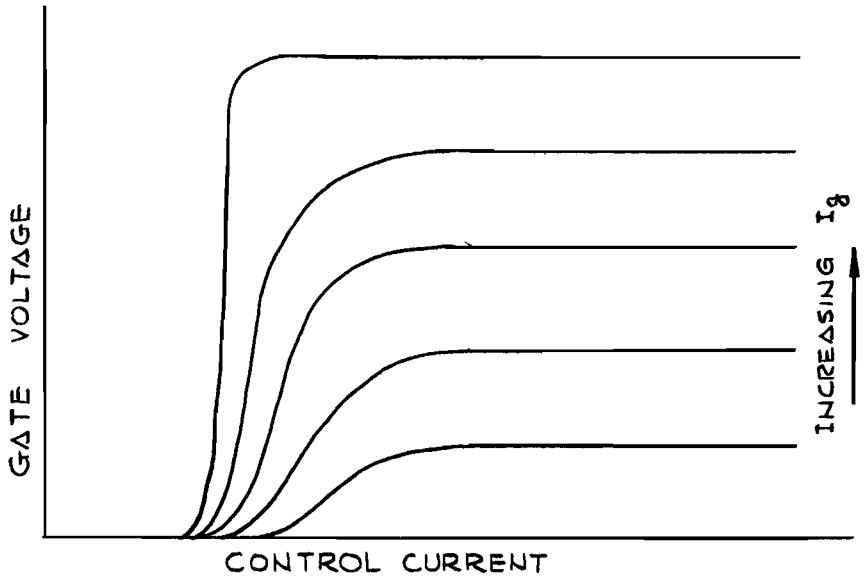

Fig. 5

Voltage Transition Curves

For a large control current its field dominates and only small gate currents are sufficient to quench the gate. On the characteristic curves this appears as the normal resistance curve. As the control current is decreased, the self-field of the gate, that is, the magnetic field due to the gate current, predominates and the slope of the characteristic curves changes from that of normal resistance to horizontal lines as shown in Fig.4. The mechanism in the interior of the gate responsible for this behaviour is explained in the chapter dealing with hysteresis.

The device symbol for the wire-wound cryotron is defined in Fig.6 where C-C and G-G are the control and gate terminals, respectively. I_c, I_g, V_c and V_g are the d-c control and gate currents and voltages, respectively. Lower case letters are used for a-c values.

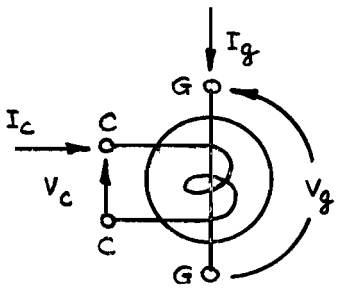

Fig. 6
Symbol of Wire-Wound Cryotron

Using the same physical arrangement as Buck(0.009 inch Ta gate, 0.003 inch Nb Control), Parkins (7) investigated the cryotron as a possible amplifier, obtained some static characteristic curves, and upon synthesizing his experimental results, derived the small signal model shown in Fig. 7. The current gain parameter, α , did not contain any inductive coupling effect.

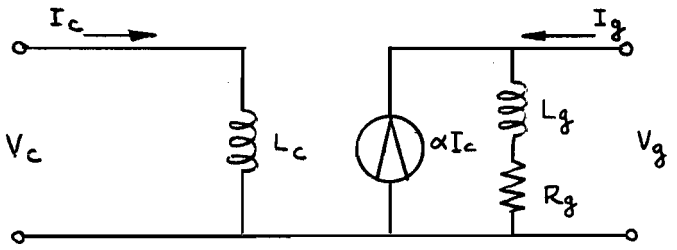

Fig.7
Small Signal Model for the Cryotron
as an Amplifier

Chirlian, who was Parkins' research director, and Marsocci (8, 9, 10, 11, 12) used Parkins' experimental results to expand the theory of the cryotron as a linear amplifier. They derived gain expressions for various connections of the control and gate, and gave expressions for optimized gain parameters. Among the uses of the cryotron they proposed application as an operational amplifier.

Tantalum, although very convenient when working at 4.2 $^{\circ}$ K, because of its low value of H_c, often shows an erratic behavior in the transition region. If the cryotron is used as an amplifier, then the transition region should be as broad as possible. An alloy of lead and indium has this characteristic, plus the additional property that the transition temperature can be varied by changing the composition of the alloy. It has been investigated by a number of workers (13, 14) for low temperature application, and Gygax (15) used it in his superconducting d-c amplifier.

The major application of the cryotron is as a switching device, and the switching time is determined by the ratio of the control inductance to the normal gate resistance. An improvement in this ratio can be achieved by decreasing the gate diameter since this diminishes the control inductance and increases the gate resistance. There are, however,

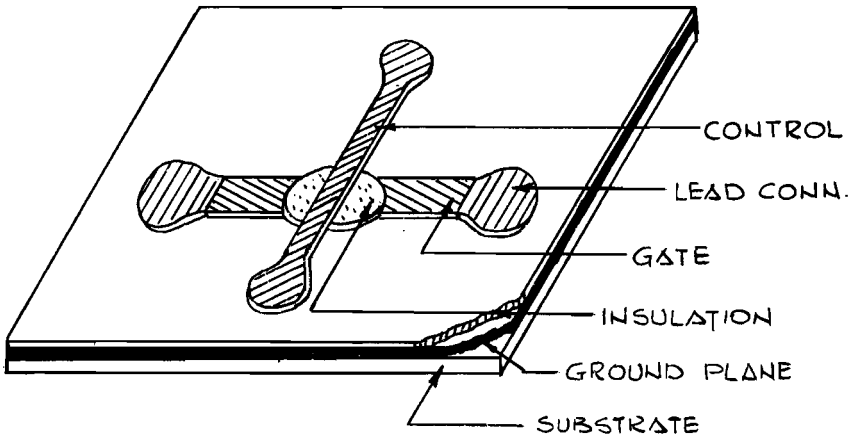

Fig. 8
Crossed-Film Cryotron

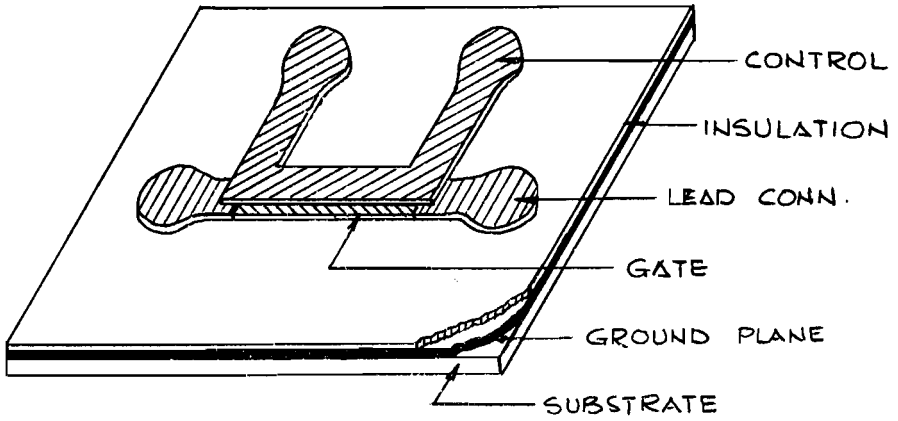

Fig. 9
In-Line Cryotron

practical limitations to the size of the wire and very small switching times can never be obtained with the wire-wound cryotron.

In the thin-film cryotron the gate and control are deposited in the form of thin, narrow films, reducing the control inductance and thus decreasing the time constant markedly. If the control is deposited perpendicularly to the gate the crossed-film cryotron is formed; if they are parallel, the in-line cryotron results, as shown in Figs. 8 and 9.

The magnetic field that is instrumental in quenching superconductivity in the gate is due to the currents in the control and the gate.In the wire-wound and crossed-film cryotrons the two fields are perpendicular to one another, so that the direction of the currents is of no importance, resulting in bilateral devices. In the in-line cryotron the magnetic fields due to the two currents reinforce if the currents are in the same direction, and tend to cancel for opposing currents, resulting in a non-bilateral device. Typical current transfer curves are shown in Fig.10.

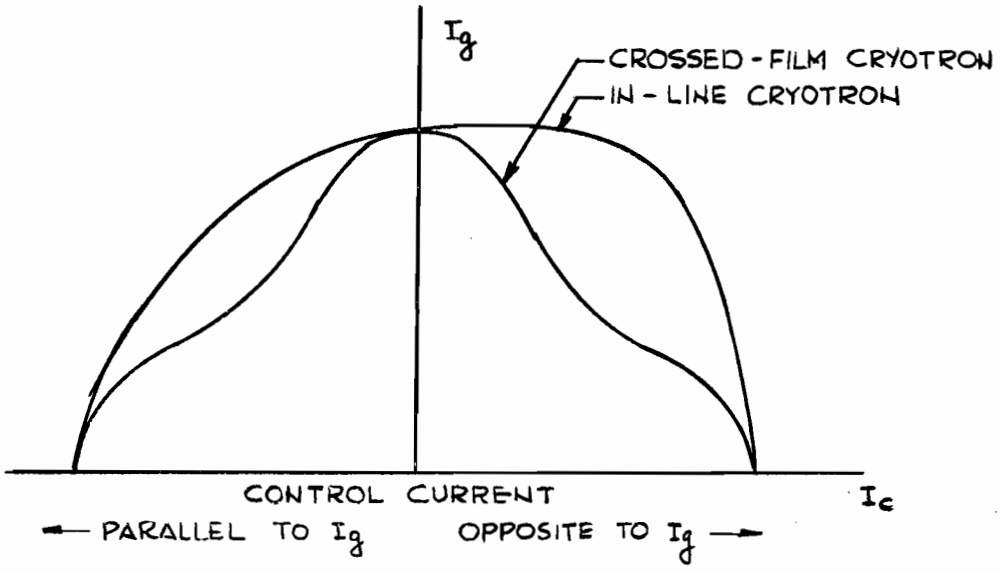

Fig. 10
Current Transfer Curves
for Crossed-Film and In-Line Cryotrons

Richards (16) proposed an equivalent circuit for the crossed-film cryotron as a linear amplifier similar to that used by Parkins.

3. The Intermediate State of a Superconductor

Of particular interest in the application of a cryotron as an amplifier is the intermediate state of the superconductor. This is the most non-linear region in which the material undergoes the change from the S to the N-state or vice versa, and it is in this area that the cryotron operates. In the N-state $B_i = \mu H_a$ and in the S-state $B_i = 0$, where B_i is the magnetic induction inside the superconductor and H_a is the applied magnetic field. The intermediate state is then defined as that region in which $\overline{B_i}$, the average value of B_i, is

$$0 < (\overline{B_i}) < \mu H_a \qquad (2)$$

The transition from the S to N-state occurs abruptly only if the specimen is very pure, long, cylindrical and placed in a longitudinal magnetic field. In this special case the demagnetizing coefficient is zero and the critical magnetic field is reached simultaneously all over the surface. In this work the field is not longitudinal, but is the resultant of the field due to the control current (longitudinal), and that due to the gate current (circular). As the resultant field is increased the superconductor enters the intermediate state and breaks up into a series of normal and superconductive regions or domains. How this comes about can be seen by the following simple argument.

One of the fundamental properties of a superconductor is the exclusion of a magnetic field from the body of the material when it is in the S-state. A magnetic field can only penetrate to a very shallow depth of about 10^{-5} cm, known as the penetration depth, if the dimensions of the material are large compared to the penetration depth. The distribution of the field around the material, when it is in the S-state, is shown in Fig.11(a), where it is obvious that the lines of force

concentrate most strongly at points A and B.

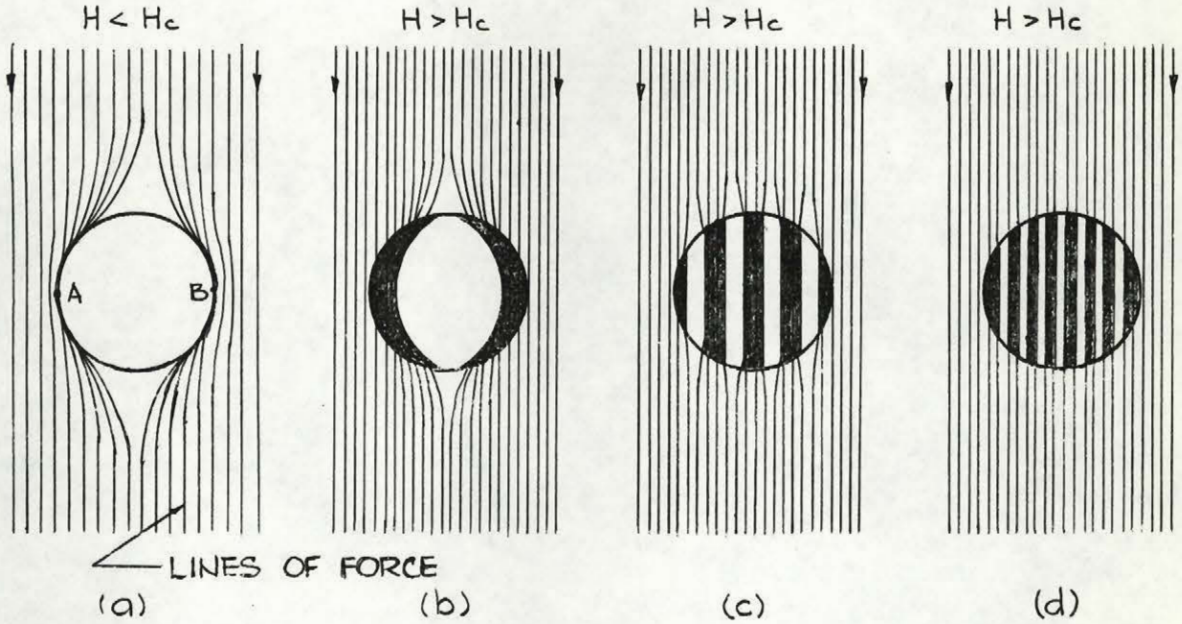

Fig. 11
Penetration of a Magnetic Field
into a Superconductor

Upon increasing the field, the value H_c is first reached at these two points forming N–regions there, and if the resultant N - S domains were to take the configuration in Fig.11(b), then at the N - S boundary a field of H_c is required to retain the shaded segments in the N-state. However, because the lines of force strive for a minimum magnetic field energy, they tend to be as little distorted as possible and the greatest concentration of them will be at the N - S boundary, leaving the field in the region between the boundary and the surface of the material at a value less than H_c. This shaded area can thus not be normal and the configuration in Fig.11(b) is not stable. To achieve a more favorable field energy, that is, as little distortion of the lines of force as possible, the N and S–domains could be formed throughout

parts of the material as shown in Fig.11(c). In this simple picture the energy can be further minimized by a second subdivision of the N-domains as in Fig.11(d).

For a minimum distortion of the magnetic field very many N-domains should be created, but this requires the formation of many walls between the N and S-regions. It requires energy to create a wall (17) and it is this energy that limits the smallness of the N-domains. Although small domains are energetically more favorable for the magnetic field, an equilibrium condition is reached between the field energy gained and the wall energy expended in producing new domains.

Domains have been observed experimentally by many workers (18,19,20,21,22,23). Meshkovskii and Shal'nikoff measured the magnetic field in a narrow slot cut into a superconductor and then on the surface directly with the aid of a bismuth probe. From these field measurements topological maps were drawn of the surface of the superconductor which showed irregularly shaped regions of N and S-domains. It was noticed that the intermediate state was almost exactly reproducible at different time intervals. If the specimen was allowed to warm up and was then recooled and remeasured, a very close agreement between results occurred. This suggests that the configuration is not an accidental arrangement, but is influenced by the properties of the material such as purity, stresses, or crystal orientation.

In his investigations, Schawlow used the powder technique in which a finely ground powder of niobium is sprinkled on the surface of the specimen. Niobium was chosen because it is superconducting at all times at the temperature and magnetic fields of interest. It is then a perfect diamagnet and is expelled from the surface of any N-domains, since these contain a magnetic field, but will remain on the S-domains, so that a photograph will clearly show the domain structure on the surface.

When a magnetic field was applied perpendicularly to a disk of very pure lead a great many small N and S-domains appeared, that increased in size when impurities were added. Arc - melted rhenium displayed a similar pattern as pure lead, but when it was coldworked the domains became much larger. Upon studying the rate of advance of a normal domain in a superconducting surrounding, it was discovered that this depended on the ratio of the surface to volume of the N-domain. If its surface area is large, then there exists a long path for the eddy currents and they are quickly dissipated by the normal resistance. A magnetic field thus penetrates more quickly into a superconductor if the solid front of the N-domains breaks up, thereby increasing the surface area.

Shubnikov and Nakhutin (24) applied a measuring current to a sphere in the intermediate state and measured zero resistance in the direction parallel to the applied magnetic field, and non-zero resistance in the direction perpendicular to it. This suggests a laminar type domain structure extending across the entire specimen perpendicularly to the current flow so that no superconducting path exists for the current. This type of domain configuration was actually observed by Shal'nikoff (25). He used a cylindrical sample of monocrystalline tin and observed the domain configuration by the powder pattern technique while introducing a current into the specimen.

De Sorbo and Healy (37) give a very good pictorial representation of domains in superconducting disks for an externally applied magnetic field with no current flow. This reference contains many photographs obtained by the magneto-optic technique.

4. Experimental Techniques

The experiments were performed at 4.2°K, and at this temperature the critical magnetic field of the gate material had to be of a magnitude that could be generated by a current of about one ampere through a control winding of 400 or 500 turns.

There are several metals and alloys that satisfy this requirement, some of which are shown in Fig.12. Tantalum with an H_c of approximately 60 oersteds and two indium - lead alloys were used; tantalum was easily available, and the alloy was chosen because of the simplicity of changing the critical temperature by a variation of the composition of the two elements. The relationship between the atomic percentage of lead-in-indium and the corresponding critical temperature is shown in Fig.13 (15).

Two alloys of 9.25 and 9.5 atomic percent lead-in-indium were used. In order to obtain the desired alloy, the weight- rather than the atomic percentages are required, since the former can be weighed very accurately on a sensitive balance. The interconversion of atomic and weight percentages is given by the relation

$$x = \frac{100\ y}{y + \frac{B}{A}(100 - y)} \qquad (3)$$

where x is the percentage by weight and y is the percentage by atoms of the element that has atomic weight A in a binary alloy with another element of atomic weight B.

The indium - lead alloy was cast into a slug and then extruded into a 0.013 inch diameter wire in an extrusion press shown diagrammatically in Fig.14. Due to the small diameter of the opening in the die, it was necessary to heat the press and slug by a contact heater to 100°C before applying pressure by means of a hydraulic press.

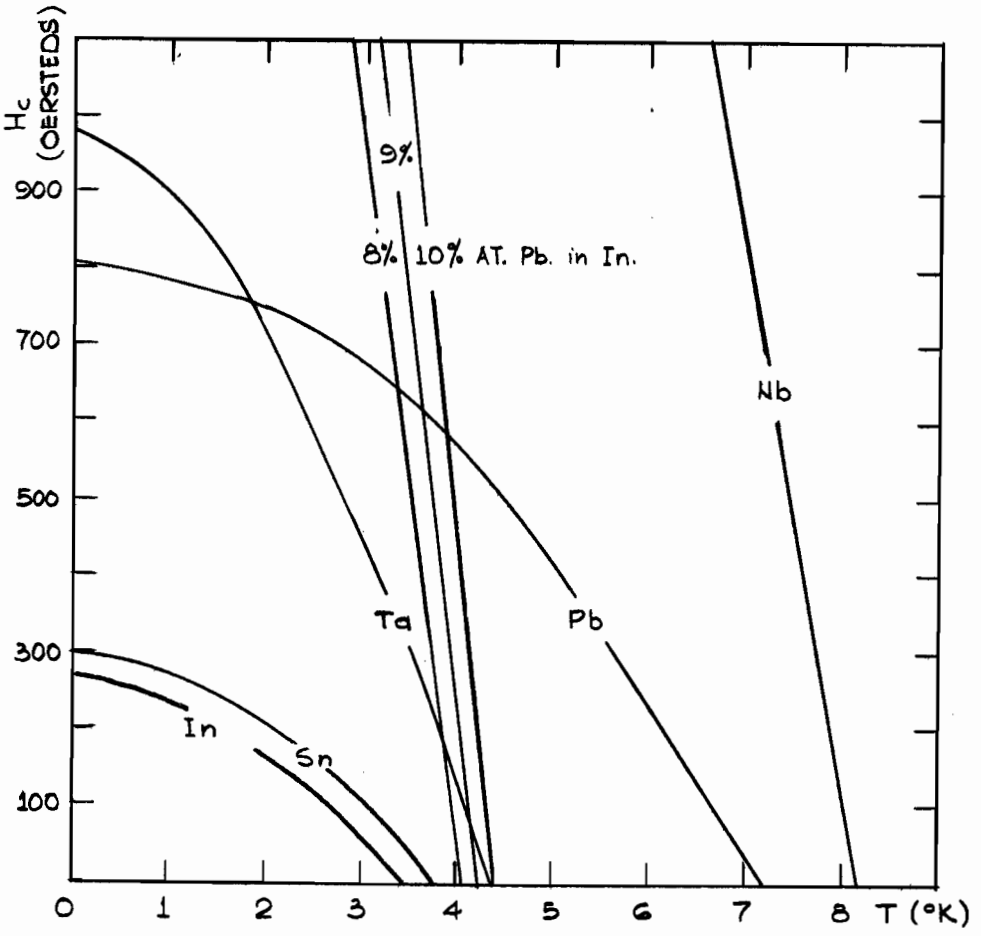

Fig. 12

Critical Magnetic Fields

as a Function of Temperature

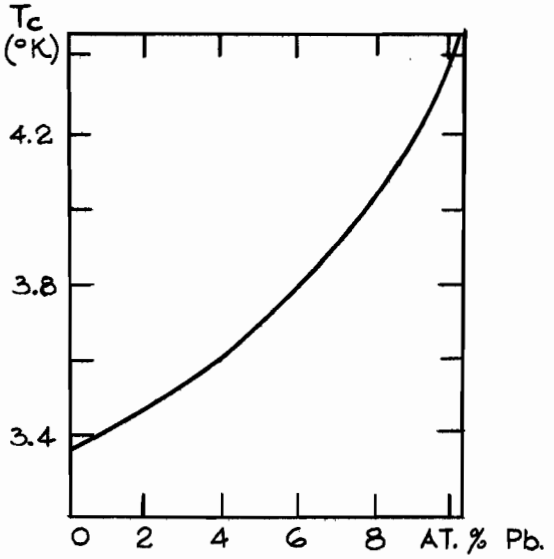

Fig. 13

Atomic Percent Lead-in-Indium

as a Function of Critical Temperature

Lead and indium were supplied by the Fisher Scientific Company in the following purities:

lead - 99.999%
indium - 99.99 %

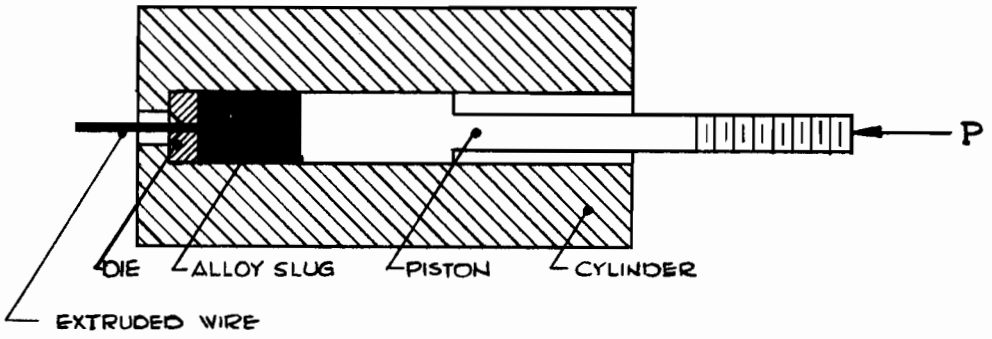

Fig. 14
Extrusion Press

For the control winding, niobium and a lead - tin solder wire, both of 0.005 inch diameter, were available. Although copper is not a superconductor, a 0.003 inch copper wire was used for the sole reason that its diameter was smaller than the above. Its resistivity at 4.2°K was measured to be 2.3×10^{-8} ohm-cm, resulting in a typical control winding resistance of 30 milli-ohms. At a current of 500 mA this gave rise to a power dissipation of 7.5×10^{-3} watts, evaporating a very small amount of helium (approximately 0.01 liter per hour). However, in any practical application of a cryotron the control winding would be superconductive.

To wind the control around the gate a winding mechanism was built as shown in Fig.15, but before winding the control, it was necessary to insulate the gate so that no electrical contact between it and the control existed; similarly the control had to be insulated to prevent electrical

contact between adjacent turns. For the gate insulation two layers of Q-dope - a polystyrene base insulator - were applied, allowing one layer to dry before applying the next one.

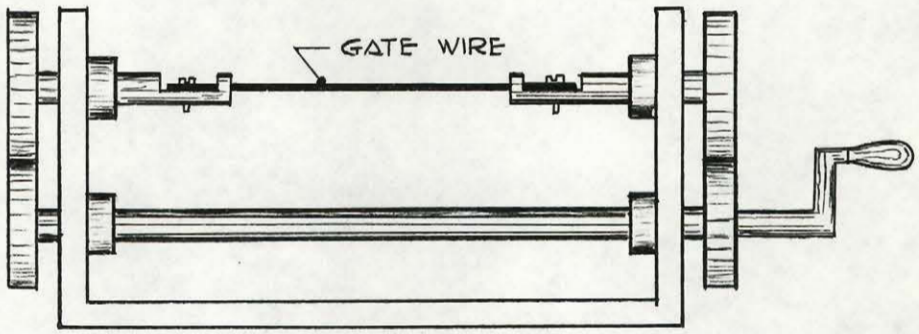

Fig. 15
Winding Mechanism

The magnetic field due to the control current is directly proportional to the number of turns per unit length. Therefore, a thin wire is preferable and the insulation covering it should be a thin coating able to withstand bending of the wire around the gate. It was attempted to coat the solder wire with Q-dope, but the insulation was very uneven, and although a cryotron was wound with this type of control it was not used. The copper wire had been insulated commercially and was quite suitable; the niobium was insulated for this work by the Northern Electric Company.

Winding the copper wire around either the tantalum or the lead - indium gate presented no problem. The niobium wire, however, was very stiff and it was impossible to wind it around the lead - indium directly. The latter was too soft and broke repeatedly, so that the niobium was first wound around a piece of copper wire of the same thickness as the gate and upon release of the winding tension, the niobium uncoiled slightly allowing the copper to be removed and the gate to be inserted.

The cryotron was attached by screws and nuts to a phenolic plate which in turn was fastened to the head plate of the cryostat by means of a stainless steel rod. Stainless steel was used for mechanical connections between liquid helium and room temperature because of its low heat conductivity. A schematic of the cryotron on the phenolic plate is shown in Fig.16, where the dotted rectangle represents the plate, and the six heavy dots the connections.

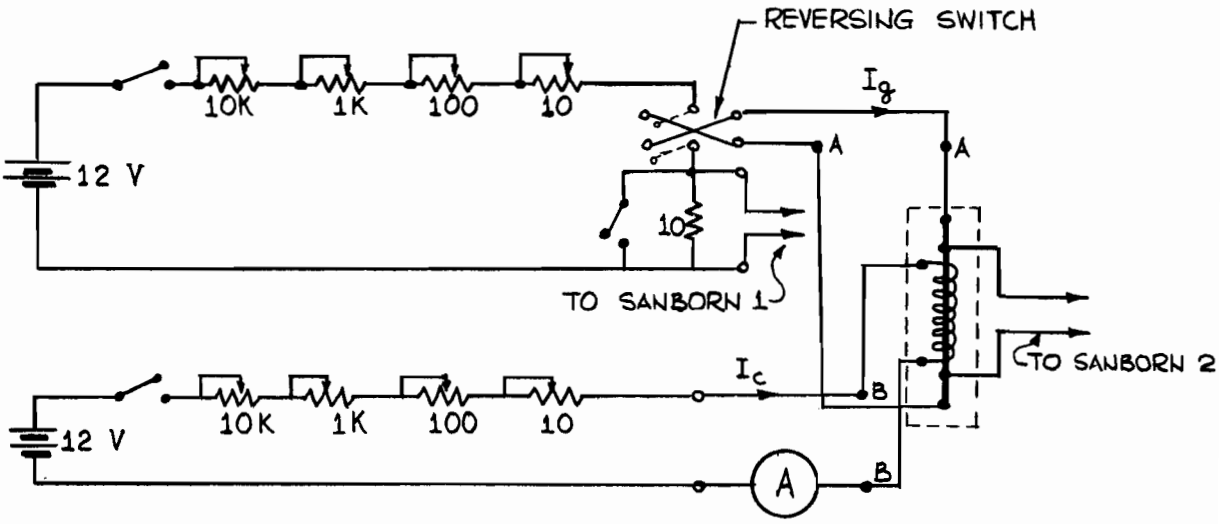

Fig. 16
D-C Measurement Circuit

Mechanical connections, rather than soldered, were used because tantalum and niobium are not wetted by solder. The lead - indium alloy has a melting point below that of ordinary lead - tin solder, so that a low melting point solder must be used. Wood's metal was used for a few connections and gave satisfactory results.

The circuit used to measure the static characteristics of the cryotron is shown in Fig.16. A calibrated ammeter measured the control current while the gate current was passed through a resistor and recorded as a voltage on a two-channel Sanborn recorder, shown as 'to Sanborn 1' in Fig.16. The gate resistance is defined as V/I, where the

voltage, V, was measured on the recorder ('to Sanborn 2'), with its highest sensitivity at 10 μV/mm, so that voltages of 10 μV could be read easily and lower ones were estimated. The gate resistances in the transition region were of the order of a few milli-ohms and were conveniently obtained by this method. Two six-volt batteries were used as power supplies and the reversing switch was provided to reverse the gate current. This, as is shown later, changes the phase shift through the device by 180 degrees.

For a-c measurements an a-c signal generator was connected between terminals A-A or B-B in Fig.16 and an oscilloscope was used for measurements. Since the cryotron offers a very low impedance, no d-c current flowed through the a-c generator and there was no need to insert a blocking capacitor in series with the generator between A-A or B-B.

The connecting wires leading into the cryostat were 26 gauge copper wire. McFee (26) has derived the following relationship between the optimum wire area, length, and current that the wire carries into the cryostat.

$$A = \frac{L\ I}{50{,}000}\ cm^2 \qquad (4)$$

where A is the cross-sectional area of the wire, L its length in cm, and I the current in amperes.

Two types of heat inflow were considered in the derivation of this equation, thermal conduction predominates if the wire is too thick and Joule heating results in evaporation of helium if the diameter is too small. However, cooling of the input leads by the helium gas was not considered, even though it reduces the heat input (27).

5. The Superconducting Ground Plane

The superconducting ground plane is widely used in cryotron operation. It is usually a sheet of lead with an H_c higher than that of the gate material, and must be of a thickness that is large compared to the penetration depth. In this work, the plane was a 0.02 inch thick sheet of lead insulated with a layer of Krysol - a spray insulator. Polystyrene Q-dope was not suitable, for it peeled off after immersion in liquid helium.

Figs.17(a) and 18(a) show the characteristic and resistance transition curves for a cryotron with a 0.022 inch tantalum gate and a 0.003 inch copper control winding of 500 turns. They were measured with the device fastened to the phenolic board directly.

The cryotron was then placed upon the ground plane which was subsequently attached to the board and pressure was applied to make better physical, but not electrical contact between the cryotron and the ground plane. The two sets of curves were remeasured and are shown in Figs. 17(b) and 18(b). Fig.19 is a comparison of two of the characteristic curves for both physical situations. It shows clearly that for a control current of 400 mA, a value such that the gate is normal for all gate currents, there is a very slight difference in normal resistance with or without the ground plane. However, for a 200 mA control current there is a very large shift of the characteristic curves, a shift that is also exhibited by the resistance transition curves in Fig.20.

The magnetic field necessary to drive the gate resistive is independent of the physical arrangement. But, as is quite evident from Figs.19 and 20, the currents required to generate this field change with the experimental arrangement. To drive the gate into the intermediate state

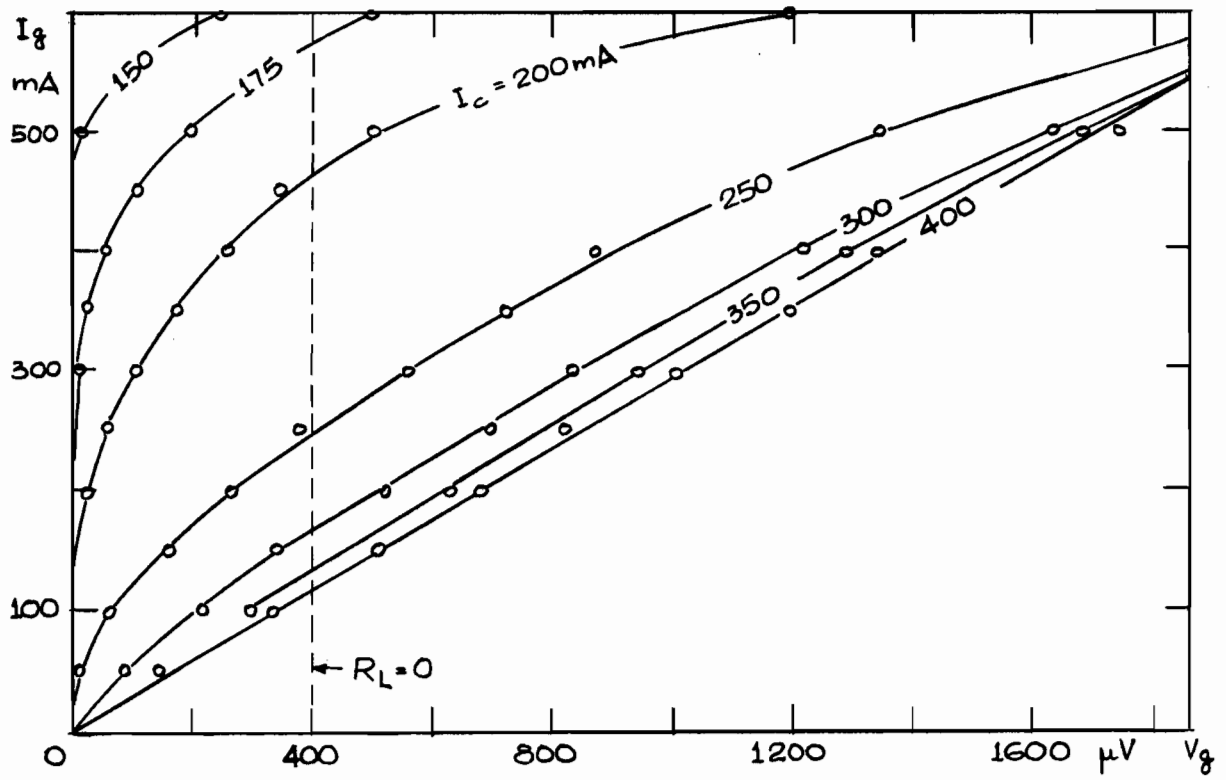

Fig. 17(a)

Characteristic Curves without Ground Plane

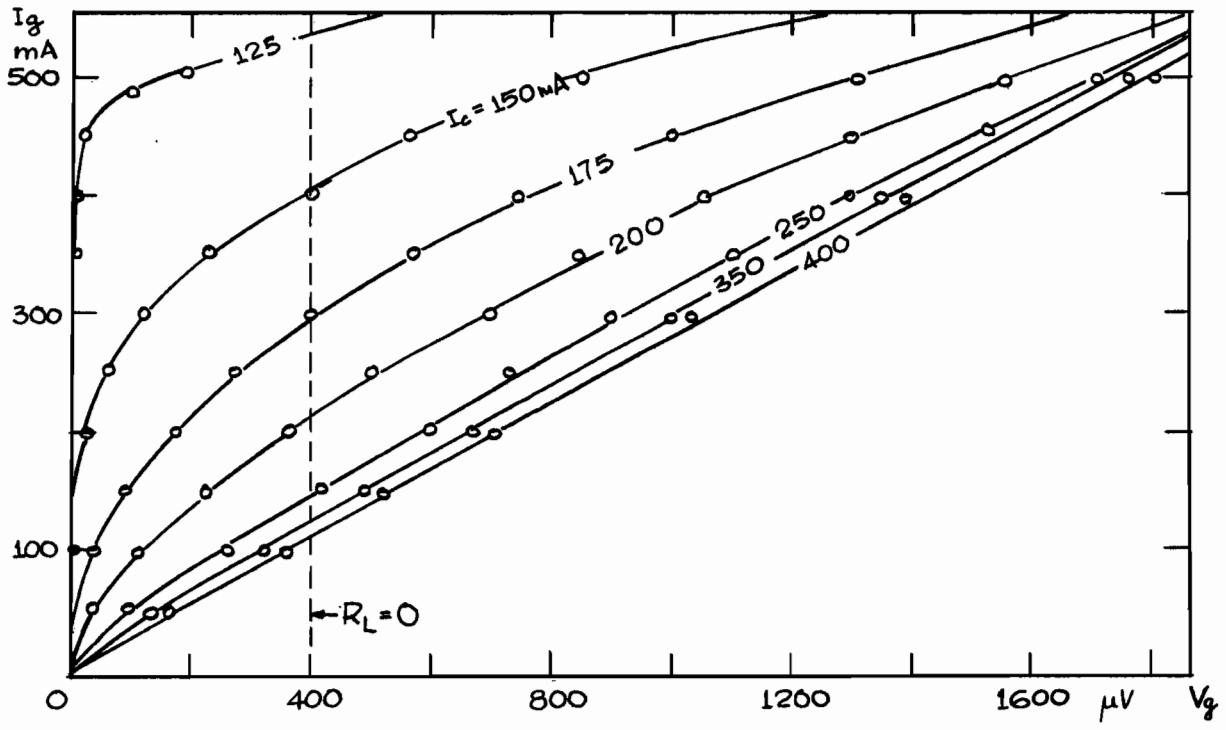

Fig. 17(b)

Characteristic Curves with Ground Plane

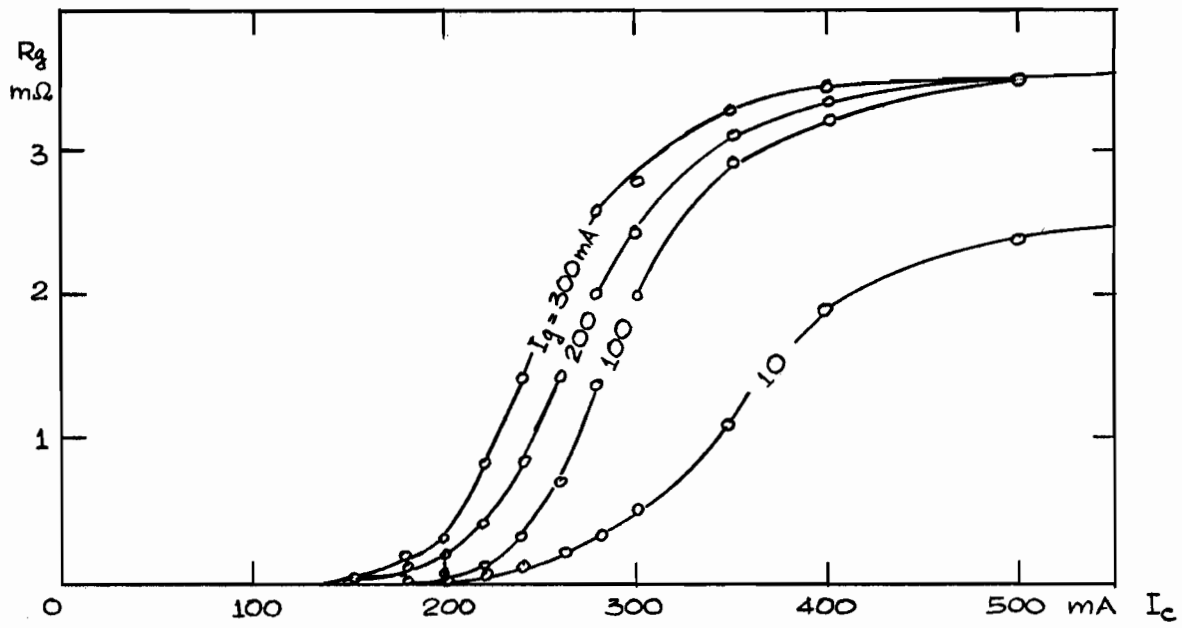

Fig. 18(a)
Resistance Transition Curves
without Ground Plane

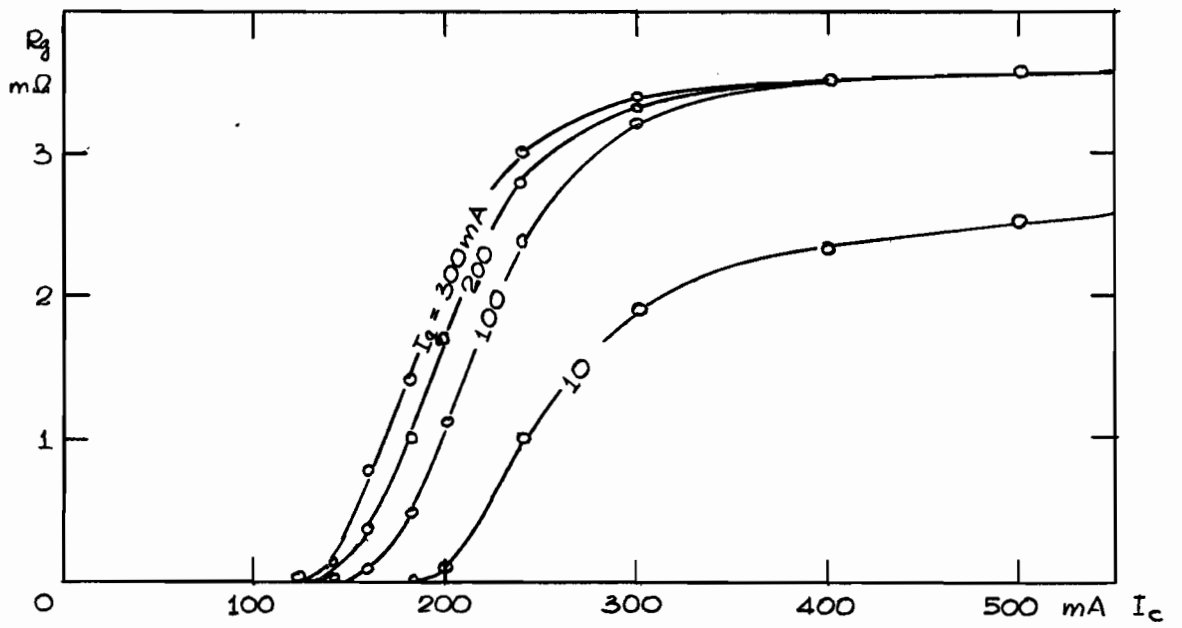

Fig. 18(b)
Resistance Transition Curves
with Ground Plane

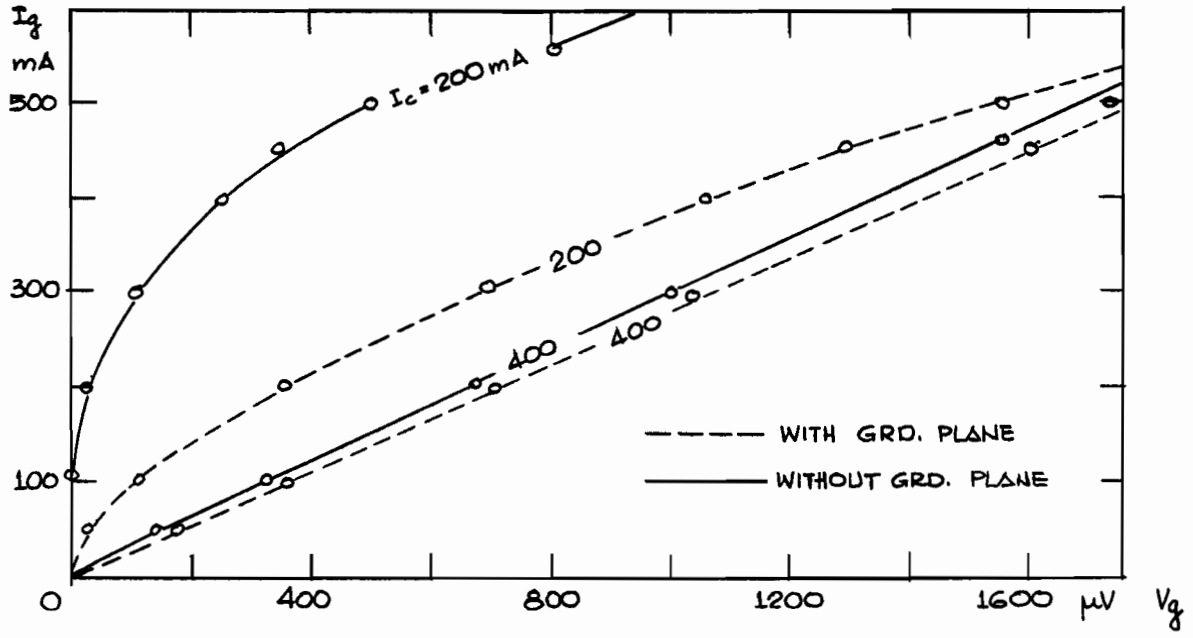

Fig. 19
Comparison of Characteristic Curves

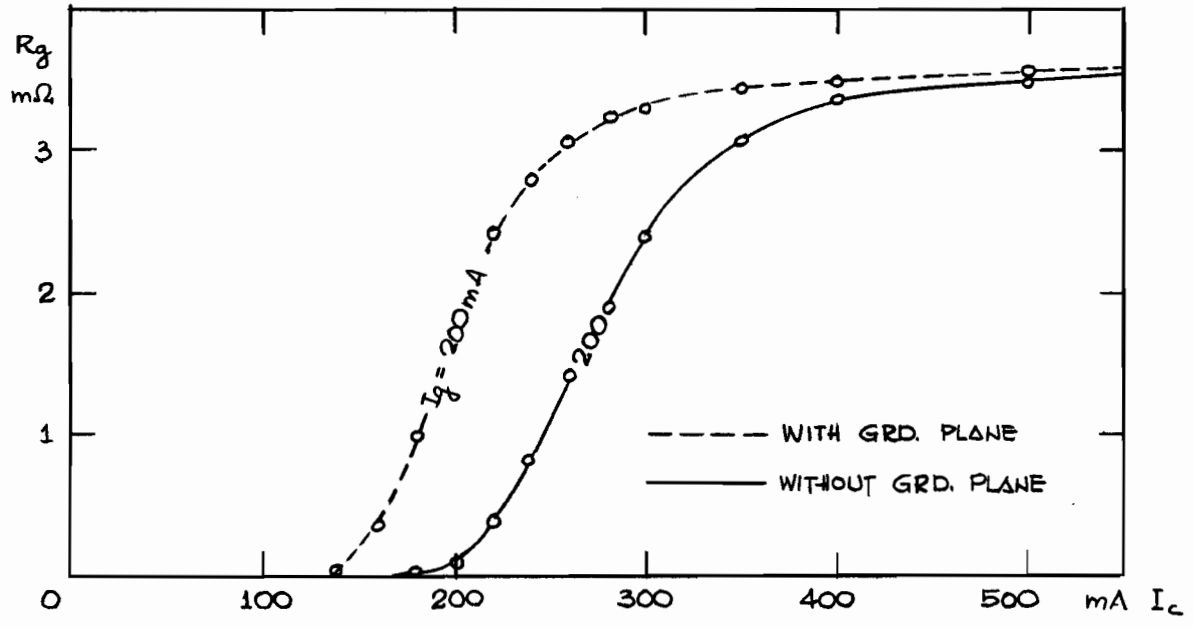

Fig. 20
Comparison of Resistance Transition Curves

such that the gate resistance is 2 m-ohms, for example, requires a certain value of magnetic field. This can be achieved by either holding the control current constant and varying the gate current as shown in Fig.19, or vice versa as shown in Fig.20. The results obtained from these curves are tabulated in Table I.

I_c (mA)	I_g (mA)	Experimental arrangement
200	600	No ground plane
200	250	Ground plane
280	200	No ground plane
220	200	Ground plane

Table I

The control current only varies between 220 and 280 mA for constant gate current, but the latter changes from 250 to 600 mA for constant control current, showing that the ground plane affects the self field of the gate to a greater extent.

A current-carrying conductor generates a self-magnetic field as shown in Fig. 21. When a superconducting ground plane is placed near the conductor, the magnetic field in the region A-B in Fig.22 will be distorted, because the magnetic field due to the current-carrying conductor will penetrate the ground plane to the penetration depth and then induce screening currents in it to prevent further penetration of the field. The contribution of the magnetic field in the region A-B due to the screening currents is equal to that field generated by an image current which is antiparallel to the external current and located the same distance, d, below the ground plane, as the original one above it. For calculation or field plotting purposes

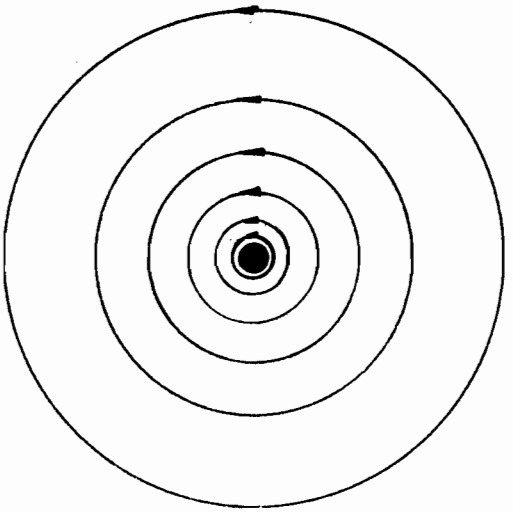

Fig. 21
Magnetic Field due to a
Current-Carrying Conductor

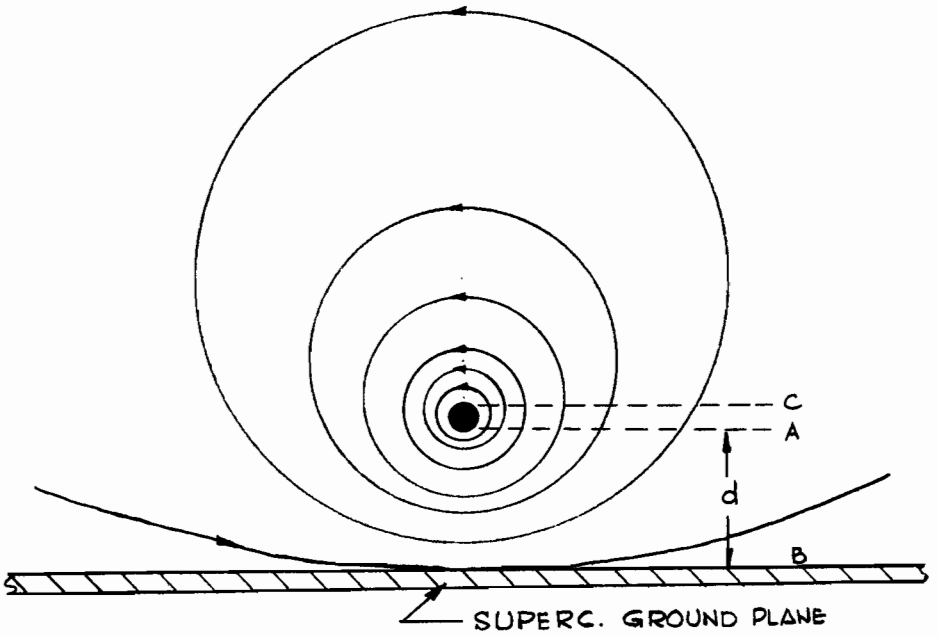

Fig. 22
Magnetic Field due to a Current-Carrying Conductor
near a Superconducting Plane

the ground plane would be replaced by the image current.

In the region A-B the two magnetic fields reinforce, but will oppose at some distance above line C. The lower portion of the conductor is thus exposed to a higher magnetic field after the addition of the ground plane.

The foregoing can be applied directly to the gate of the cryotron. Without a ground plane, a certain current, the critical current, will generate the critical magnetic field at its surface. With the addition of the ground plane the field at a portion of the surface is increased for the same current, so that clearly a current smaller than the original critical current will suffice to drive the gate into the intermediate state. This is borne out experimentally as tabulated in Table I. The fact that part of the field at some distance above the gate cancels is of no importance, since this part of the field does not affect cryotron operation.

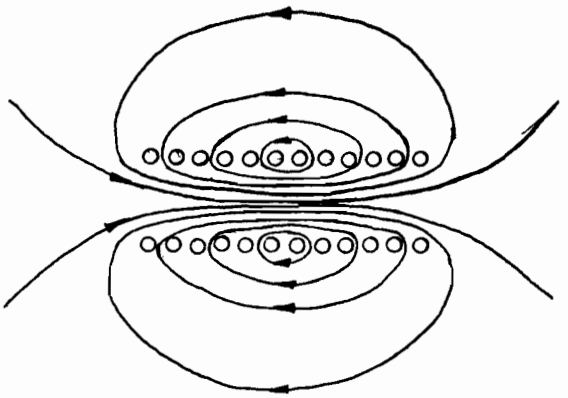

Fig. 23
Magnetic Field due to a
Current-Carrying Solenoid

The magnetic field distribution due to a current in the control winding is shown in Fig.23. Upon the addition of a ground plane, and because the cryotron is pressed against the ground plane, there is only a small gap between the lower layer of the control winding and the plane. Thus the path available for the lower portion of the field is small and the field density in the gap will be high. An easier alternate path for the field is the region above the upper layer of the winding and a possible field distribution is shown in Fig.24. The total field inside the control is unchanged, but it will distribute itself in such a way that the density in the region A-B will be higher than that in the region B-C. For a constant control current this means that the upper part of the gate will be exposed to a higher magnetic field when a ground plane is used. For a constant field a reduction in I_c is thus necessary. This was observed experimentally as shown in Table I.

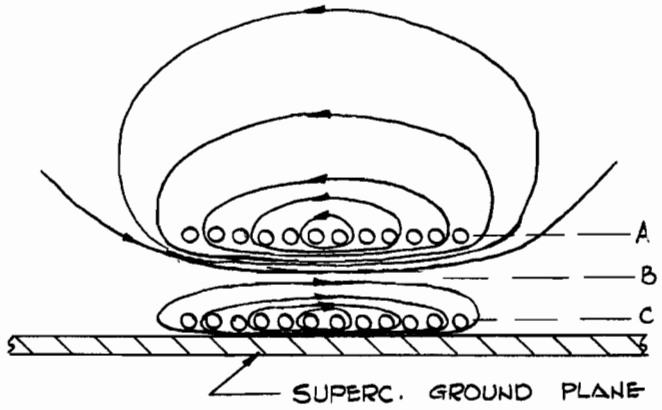

Fig. 24
Magnetic Field due to a Current-Carrying Solenoid near a Superconducting Plane

In Figs.19 and 20 the normal resistance curves do not coincide. From the slope of the curves in Fig.19 or directly from Fig.20 the normal resistances are

i. with ground plane - 3.65 mΩ
ii. without ground plane - 3.55 mΩ .

The control winding for this cryotron is 4.3 cm long. Assume that when no ground plane is present, the magnetic field required to quench the gate is confined to the length of the control, falling to a value smaller than this field outside these limits. With a ground plane, the length over which the quenching field acts is extended slightly, because the plane tends to concentrate the field for a small distance past the extremeties of the control. The effective length of application of the field is $4.3 \times 3.65/3.55 = 4.4$cm, which is one millimeter longer than without the ground plane, and an increase of this magnitude seems quite feasible with this arrangement.

The current transfer curves are curves of gate current plotted against control current. They are obtained from the characteristic curves. Fig.25 shows two of these curves for a load of zero resistance, drawn as a vertical load line through $V_g = 400\mu V$ in Figs.17(a) and (b). The shape of the curves is not changed by the ground plane. There is only a shift to smaller values of current, so that less input power is required to bias the cryotron at a certain operating point when a ground plane is used. More will be said about current transfer curves in chapter 6.

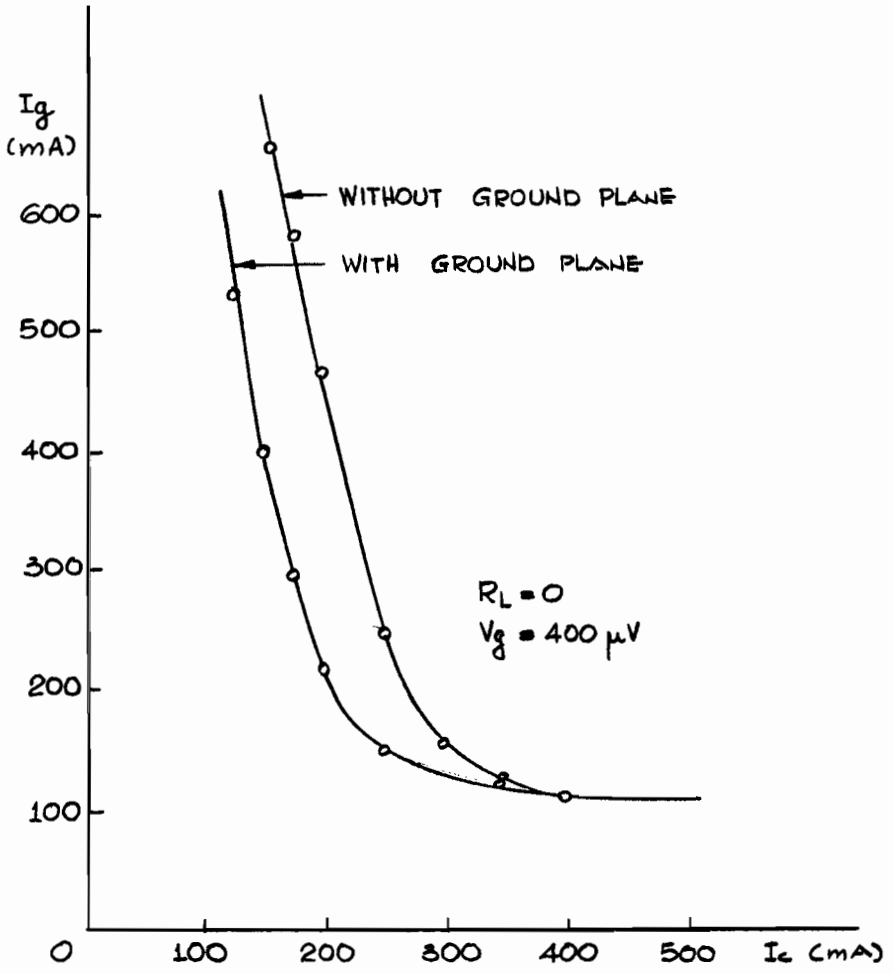

Fig. 25

Comparison of Current Transfer Curves

6. Incremental Models and Frequency Response

From the characteristic and voltage transition curves a simple incremental model can be derived. The characteristic curves give the gate current as a function of the gate voltage and control current, the voltage transition curves give the gate voltage as a function of control and gate currents,

$$i_g = f_1(v_g, i_c) \tag{5a}$$

$$v_g = f_2(i_c, i_g) \tag{5b}$$

If the operation of the cryotron is restricted to small excursions near the operating or quiescent point, then for small increments of v_g and i_c the resulting increment in the gate current is approximately

$$\Delta i_g \approx di_g = \frac{\partial i_g}{\partial v_g} dv_g + \frac{\partial i_g}{\partial i_c} di_c \tag{6}$$

The increments in i_g, v_g and i_c are given the symbols $i_{\Delta g}$, $v_{\Delta g}$, $i_{\Delta c}$. Equation (6) then becomes

$$i_{\Delta g} = g_g v_{\Delta g} + a' i_{\Delta c} \tag{7a}$$

where g_g is the incremental gate conductance and a' is the low-frequency incremental current gain parameter.

Similarly Equation (5b) results in the following relation

$$v_{\Delta g} = r_m i_{\Delta c} + r_g i_{\Delta g} \tag{7b}$$

where r_m is the incremental transresistance and r_g is the incremental gate resistance.

For a constant value of v_g, $v_{\Delta g}=0$ and from Equation (7a)

$$\frac{i_{\Delta g}}{i_{\Delta c}} = a' \tag{8}$$

and from Equation (7b)

$$\frac{i_{\Delta g}}{i_{\Delta c}} = - \frac{r_m}{r_g} \tag{9}$$

from which the current gain parameter is

$$a' = - \frac{r_m}{r_g} \tag{10}$$

The input, or control,circuit is independent of the output circuit when obtained from the static input curves, as shown in Fig.26, and is represented by a resistance which is zero for a superconductive control.

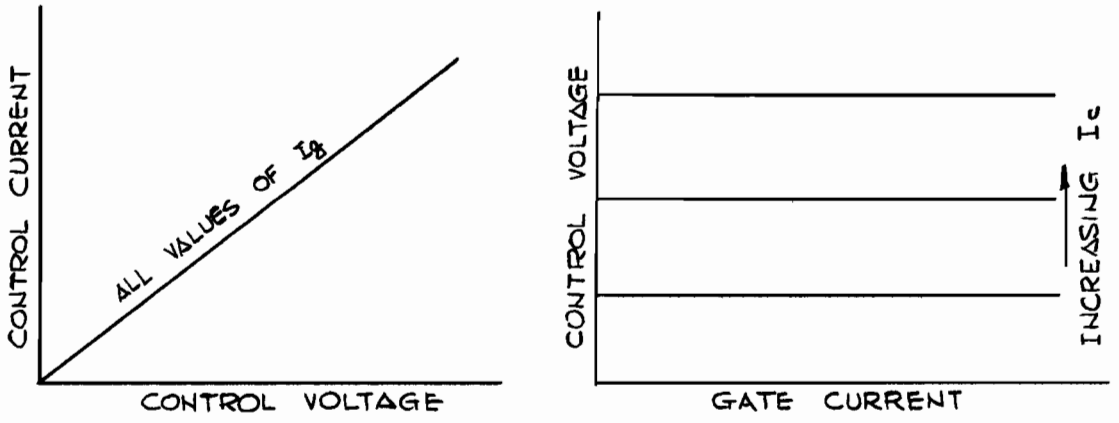

Fig. 26
Input Curves for the Wire-Wound Cryotron
with non-superconducting Control Winding

The incremental model is shown in Fig.27, but since the parameters are derived from the static curves of the device, the model is applicable only for d-c and low-frequency operation. For this reason it is designated as the simple incremental model. An improved version, to be derived later, can be applied for higher frequency operation.

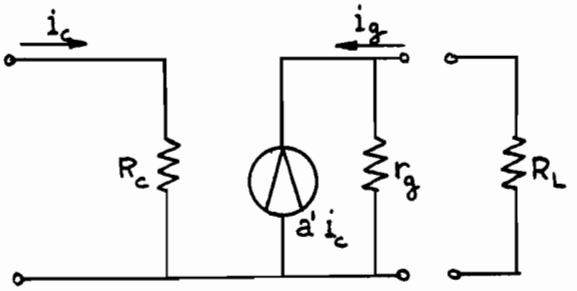

Fig. 27
The Simple Incremental Model

For a load connected across the output terminals, the current gain of the cryotron becomes

$$A'_i = \frac{-a'}{1 + R_L/r_g} \qquad (11)$$

and when $R_L=0$, the case for cascaded cryotrons where the load of one is the superconducting control winding of the next, $A'_i = -a'$, the maximum current gain.

The cryotron curves can be divided into various regions as shown in Fig.28.

Region A is the threshold region. The resistance of the gate is very small and operation in this region is not suitable, because the curves are extremely non-linear.

Region B is the saturation region. Operation is not suitable here, because the resistance of the gate is very close to its normal value, that is, the gate is almost or totally saturated.

Region C is the forbidden region. No operation is possible here, because the gate resistance would have to be larger than its normal value.

Region D is the unstable region. Since the cryotron is a current operated device it must be biased by a current, but in this region the biasing is very unstable because the Q-point fluctuates between zero and the normal resistance.
Region E is the active region and only in this region can the cryotron be operated as an amplifier.
For switching purposes the cryotron operates from region A to B, but for amplifying purposes operation is confined to region E.

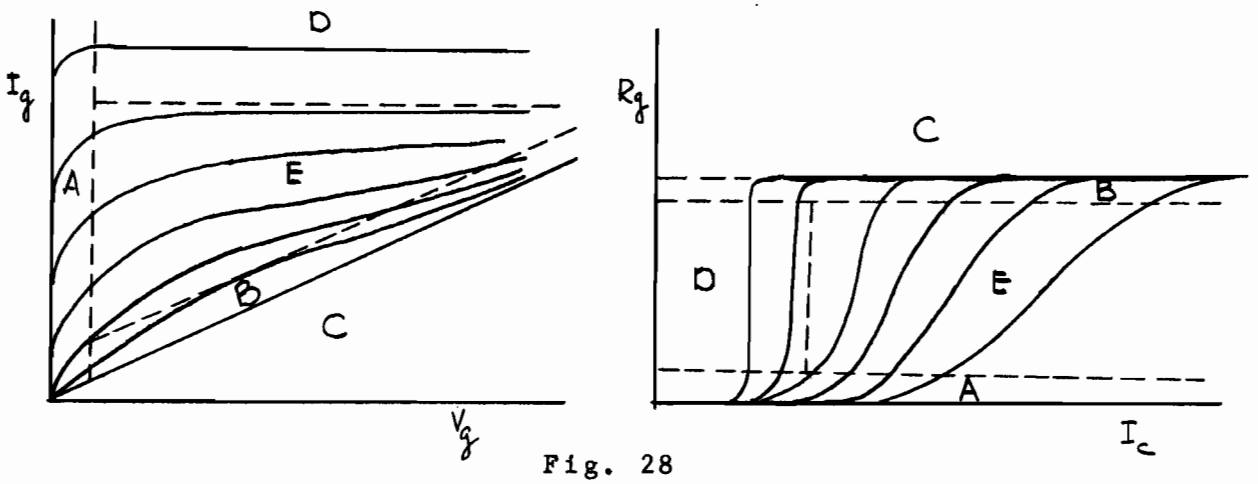

Fig. 28
Regions on Cryotron Curves

Figs.29,30,31 show the characteristic, voltage transition and resistance transition curves for a cryotron with a 9.25 at.% lead-in-indium alloy and a control of 400 turns, 0.003 inch copper wire. A quiescent point is chosen and the active region is the area surrounding this point. The excursions of an input signal will take place along a given load line. Several of these are shown in Fig.29 and it is quite obvious that unless the signal is restricted to the active region, severe distortion will take place in the threshold and saturation regions. The quiescent point is determined by the d-c bias circuit in Fig.32.

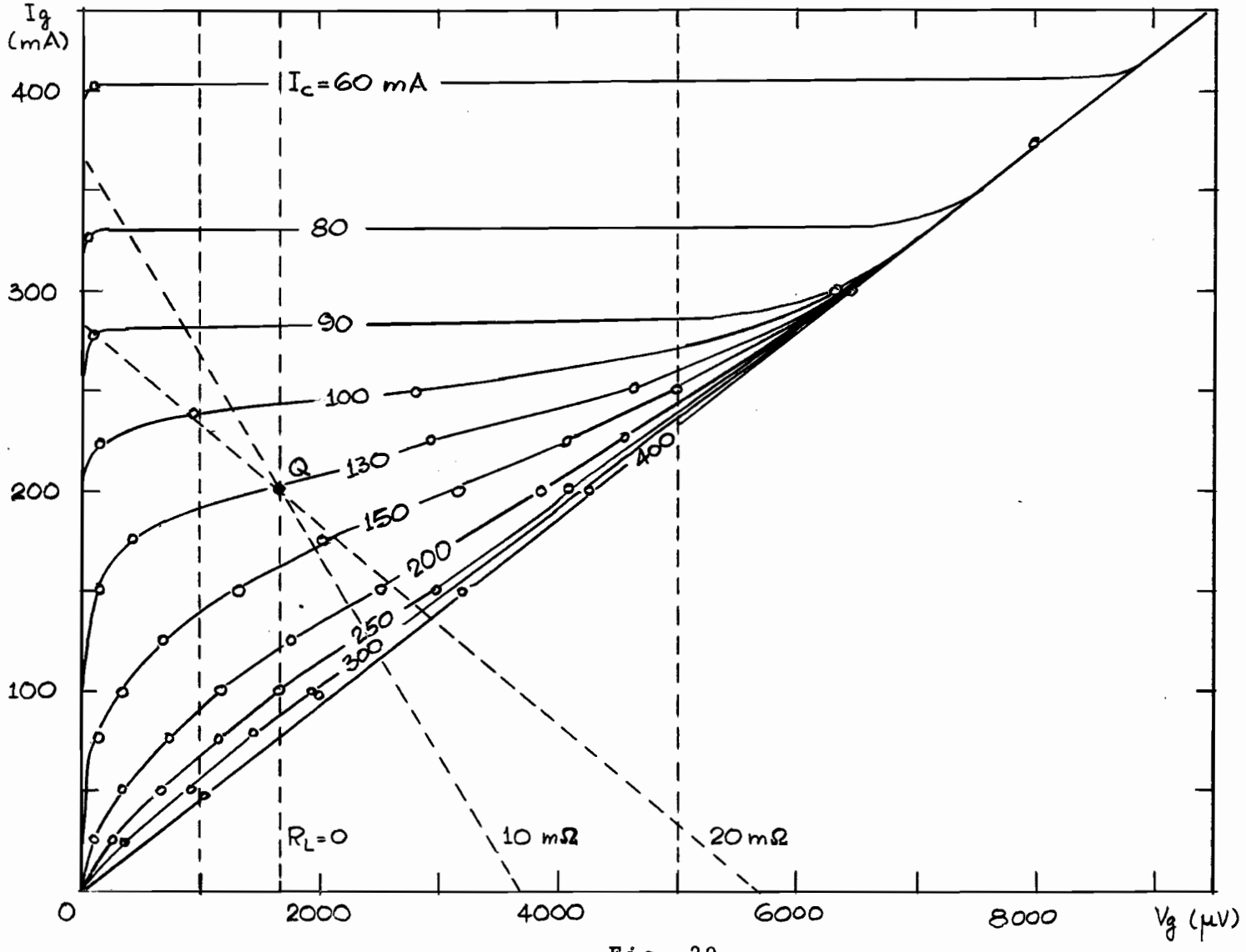

Fig. 29

Characteristic Curves

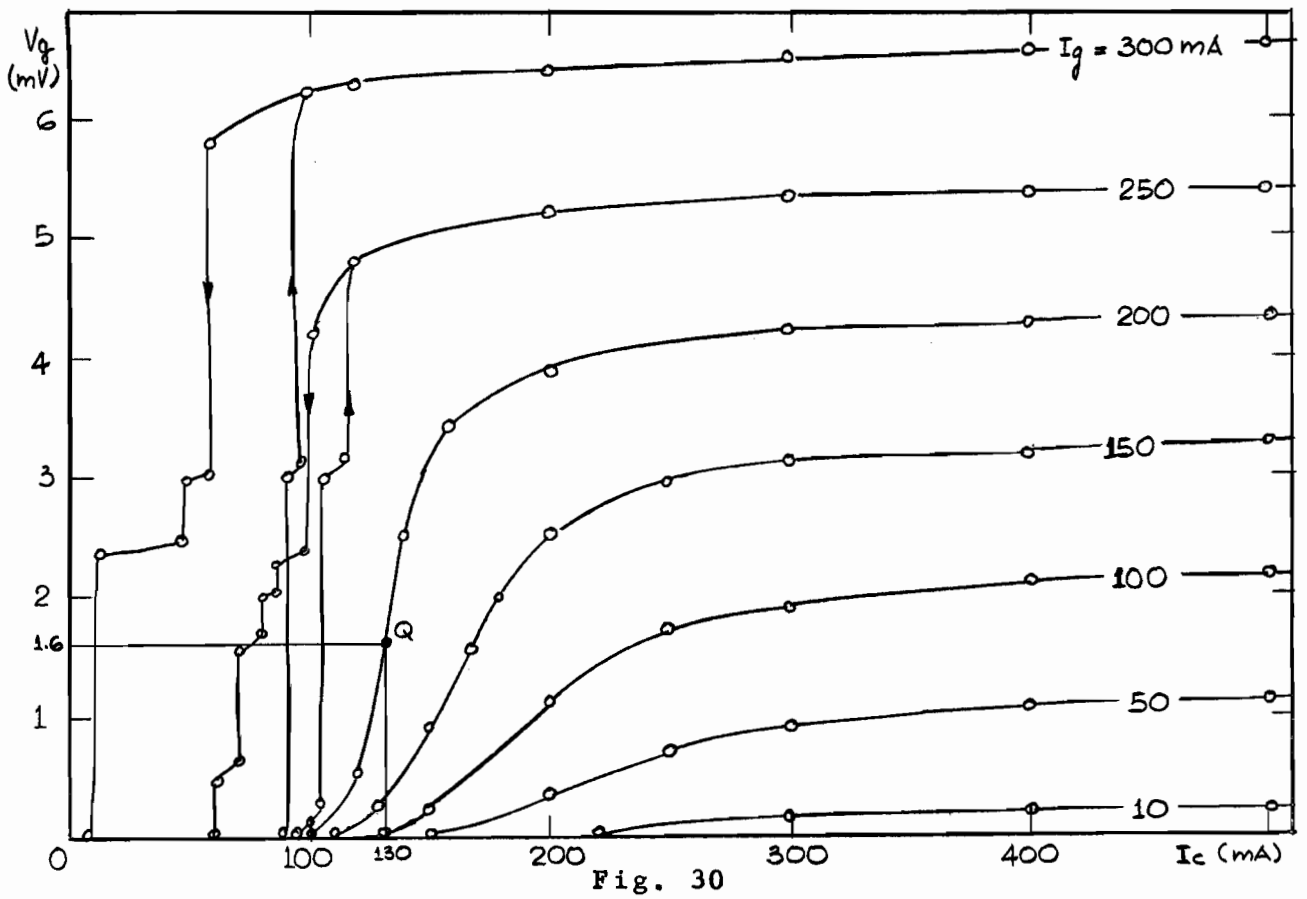

Fig. 30

Voltage Transition Curves

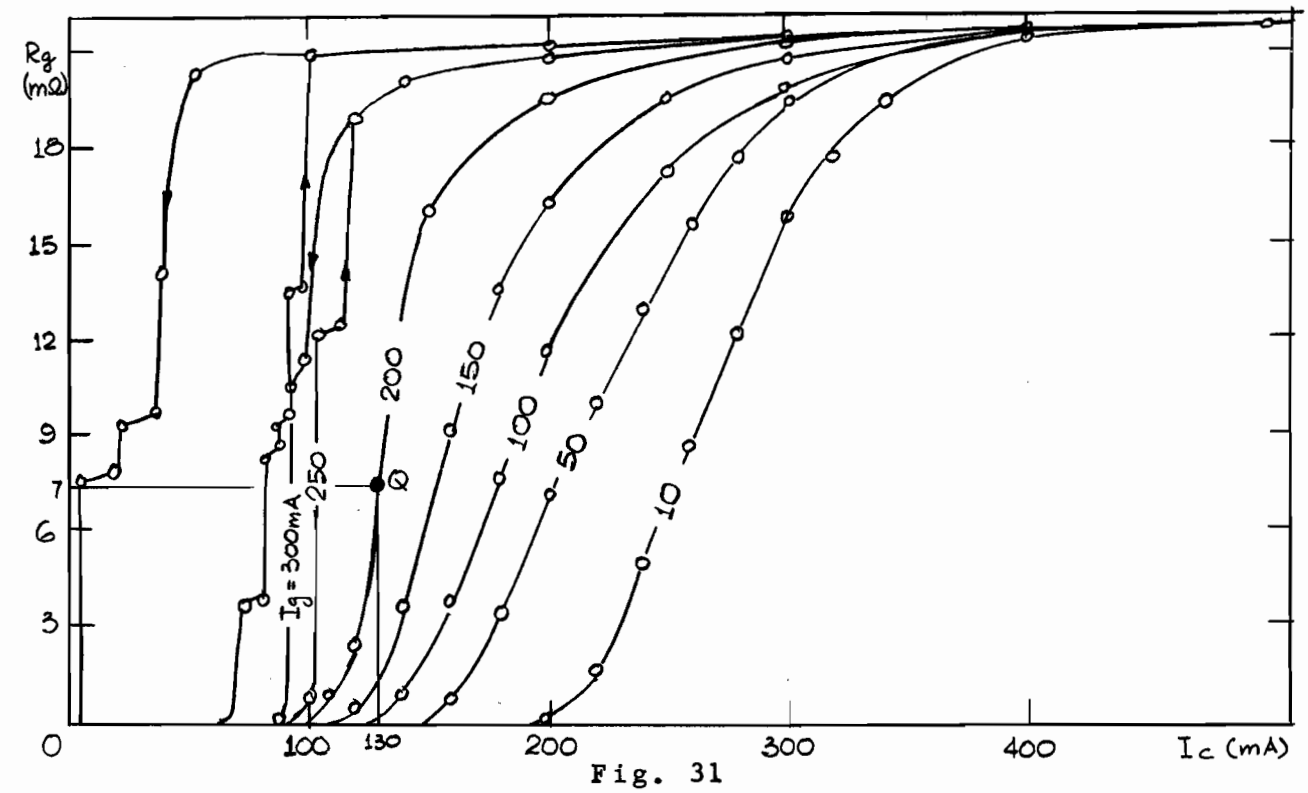

Fig. 31

Resistance Transition Curves

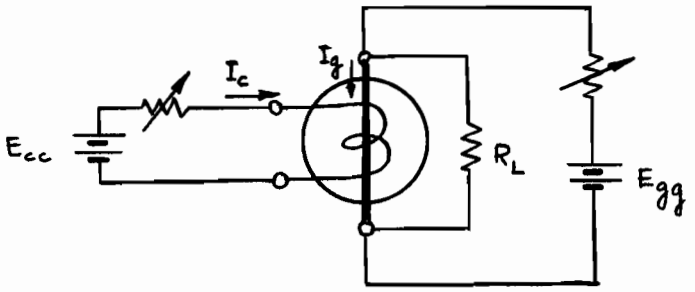

Fig. 32
D-C Bias Circuit

The manner in which amplification and distortion depend on the load resistance can be shown by the current transfer curves. Fig.33 shows a family of these curves for loads of zero resistance, that is, a vertical line is drawn on the characteristic curves (Fig.29) at a given voltage and the corresponding gate and control currents are read for points along this line. All current transfer curves originate at one point of gate current and coincide until the characteristic curves depart from the horizontal. Only the curve obtained from a vertical line through $V_g=0$ reaches the abscissa, the others cannot do this for it would entail operation in the forbidden region.

Instead of obtaining a family of current transfer curves for a zero load resistance, one can plot a set of curves for various load resistances. Fig.34 shows such a family of curves for a number of load resistances which are shown as load lines through the quiescent point in Fig.29. The slope of the transfer curves at the Q-point represents the current gain, and it is clearly seen that this changes for different loads. The parameter a' can be obtained from the slope of the curve of $R_L=0$. To show the dependence of the current gain on the load resistance, an enlarged portion of Fig.34 is shown in Fig.35.

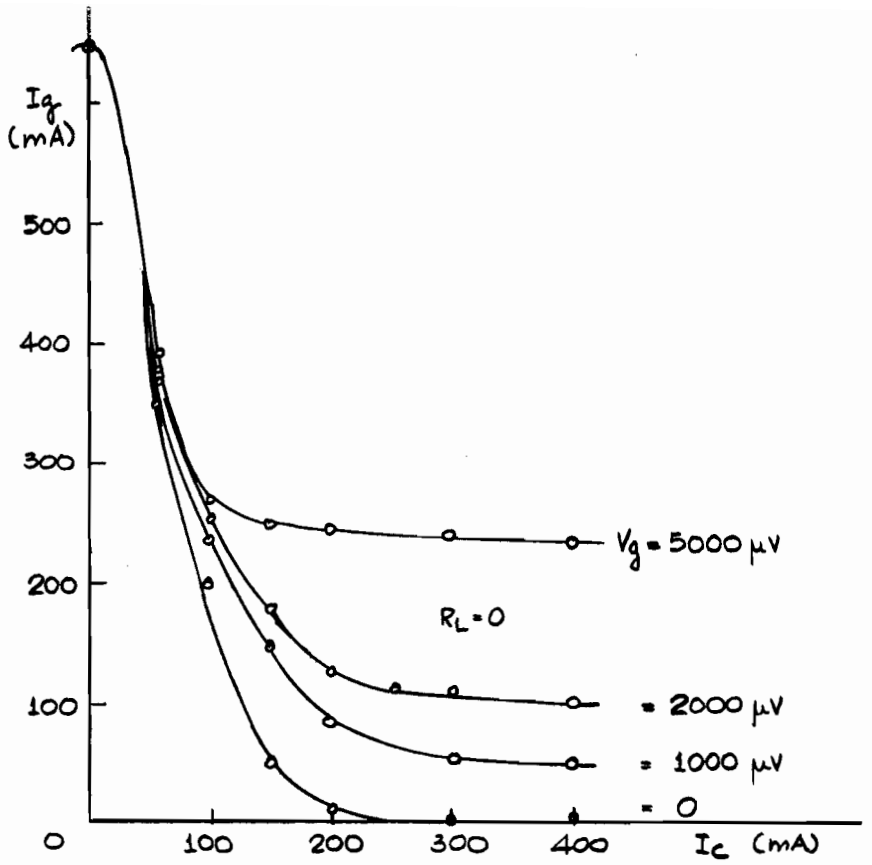

Fig. 33

Current Transfer Curves

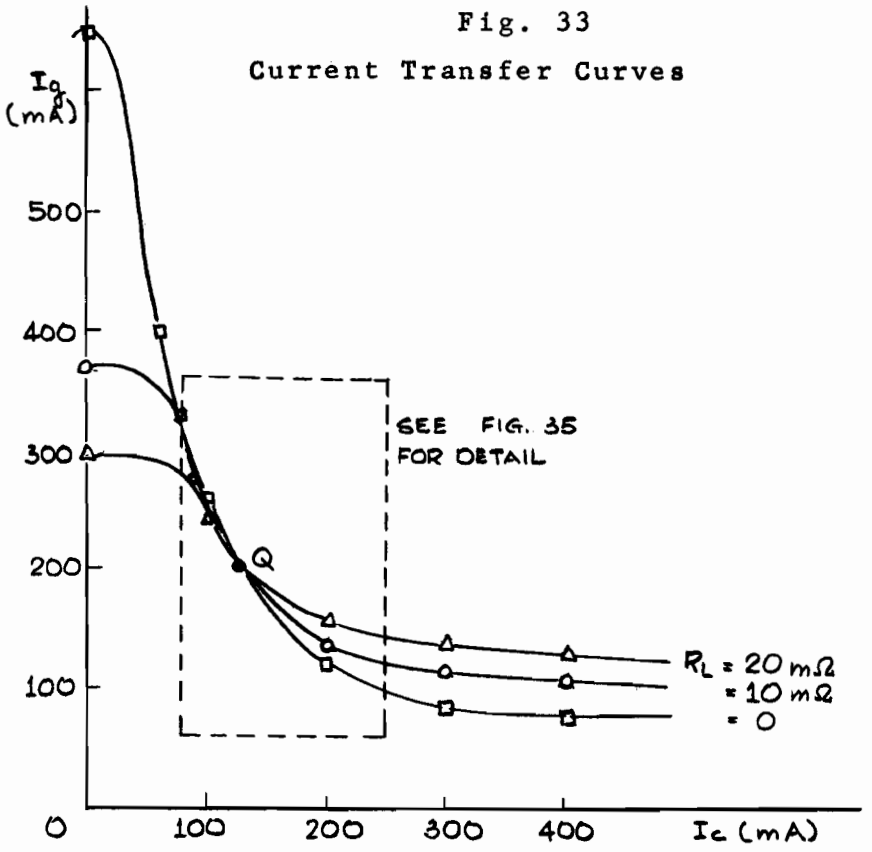

Fig. 34

Current Transfer Curves

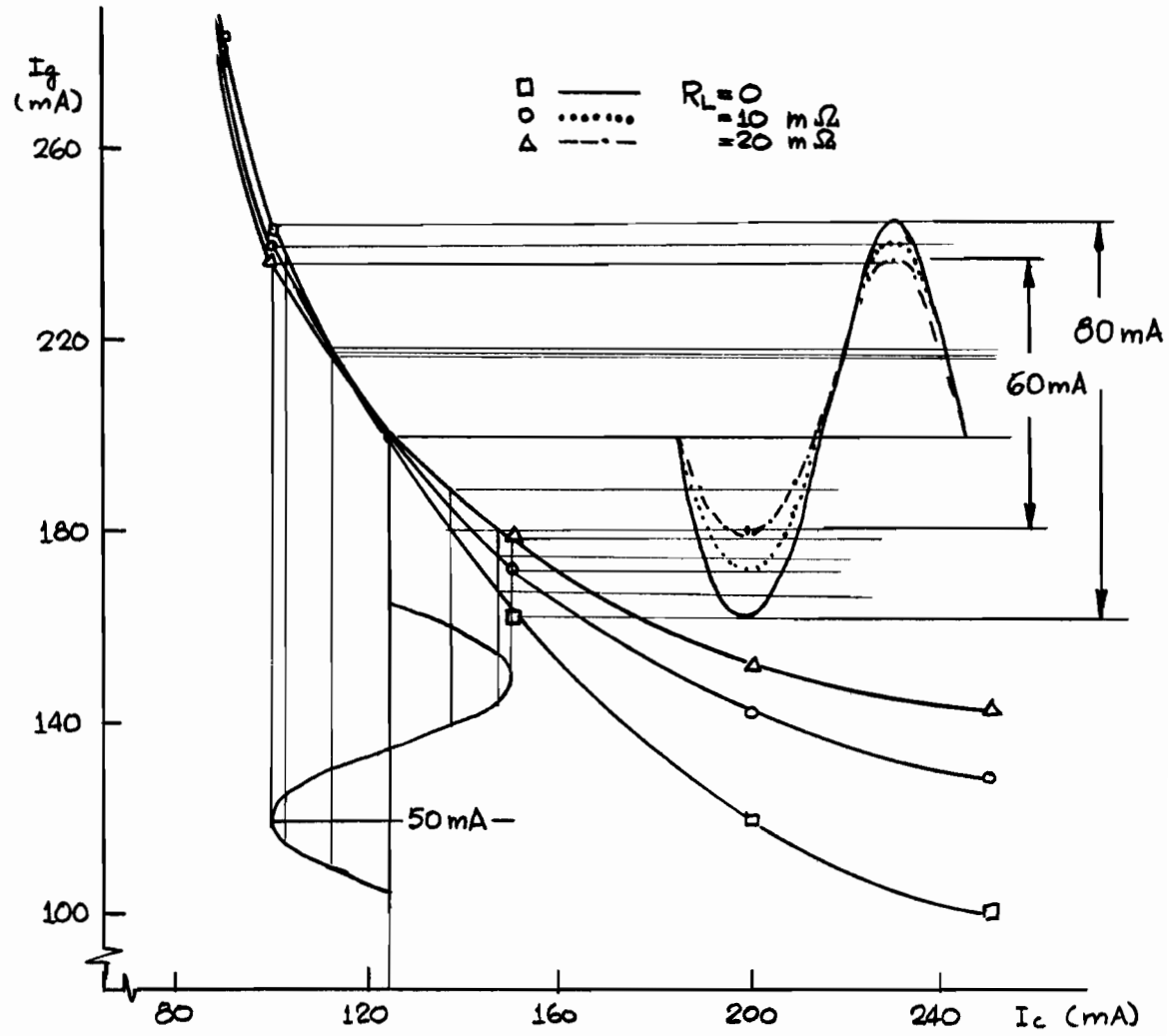

Fig. 35
Enlarged Detail of Current Transfer Curves

The wire-wound cryotron is a bilinear device and operation in all four quadrants of the current transfer curves is feasible, as shown in Fig.36. For operation in the first and third quadrant a 180-degree phase shift results between input and output of the cryotron; no phase reversal occurs in the second and fourth quadrant.

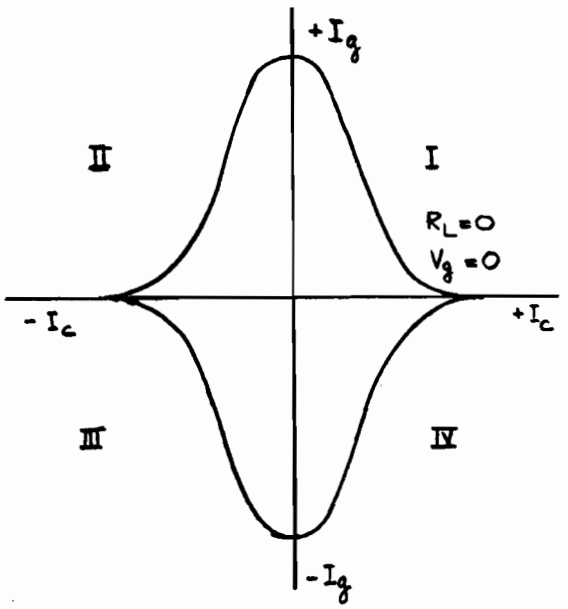

Fig. 36
Current Transfer Curves

The simple incremental model is applicable only when the input signal is d-c or very slowly varying. For higher frequencies the self-inductances of the gate and the control and the inductive coupling between these two components become important. The inductive coupling gives rise to an open circuit output voltage along the gate when an a-c control current is applied, and an open circuit output voltage along the control when an a-c gate current is applied. There is no induced voltage in the control for a d-c gate current, but a d-c control current will change the state of the gate making cryotron operation possible. The latter interaction results in a transresistance which was used in the simple incremental model.

Fig.37 shows the circuit representing the cryotron for a-c operation. L_c and L_g are the self-inductances of the control and gate, respectively, and M is the mutual inductance between the control and gate and vice versa.

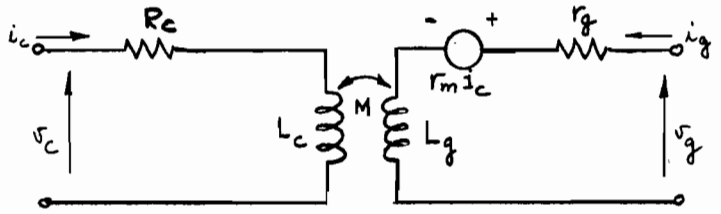

Fig. 37
Circuit of the Cryotron
for A-C Operation

For the simple incremental model the output voltage was expressed as

$$v_{\Delta g} = r_m\, i_{\Delta c} + r_g\, i_{\Delta g} \tag{7b}$$

When the self- and mutual inductances are considered, then this equation is modified to

$$v_{\Delta g} = (r_m + j\omega M)\, i_{\Delta c} + (r_g + j\omega L_g)\, i_{\Delta g} \tag{12}$$

and for constant $v_{\Delta g}$

$$a = -\frac{r_m + j\omega M}{r_g + j\omega L_g} \tag{13}$$

$$a = a' \frac{(1 + jf/f_1)}{(1 + jf/f_2)} \tag{14}$$

where $f_1 = \dfrac{r_m}{2\pi M}$, $f_2 = \dfrac{r_g}{2\pi L_g}$.

By a simple manipulation Fig.37 can be transformed into the 'improved incremental model' of Fig.38, which reduces to the'simple incremental model' of Fig.27 for low-frequency operation.

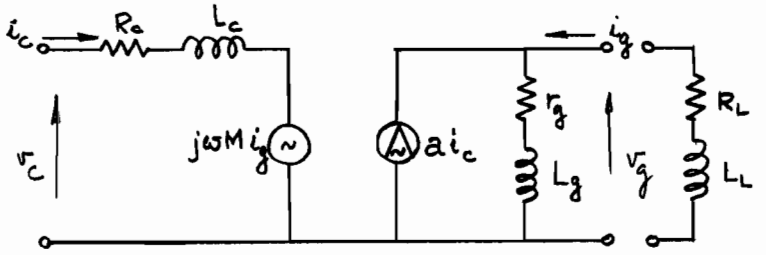

Fig. 38
The Improved Incremental Model

For a load connected across the output terminals, taking the load inductance into consideration, the current gain becomes

$$A_i = \frac{-(r_m + j\omega M)}{(R_L + j\omega L_L + r_g + j\omega L_g)} \qquad (15)$$

which can be expressed as

$$A_i = \frac{-r_m(1 + jf/f_1)}{(R_L+r_g)(1 + jf/f_3)} \qquad (16)$$

where $f_3 = (R_L+r_g)/2\pi(L_L+L_g)$. The corresponding equations for voltage+power gains are given below, where the power gain, A_p, is defined as the product $\mathrm{Re}(A_v A_i^*)$ and $f_4=R_L/2\pi L_L$ and $f_5=R_c/2\pi L_c$ (R_c and L_c are the resistance and inductance of the control).

$$A_v = \frac{-(r_m+j\omega M)(R_L+j\omega L_L)}{(R_L+j\omega L_L+r_g+j\omega L_g)(R_c+j\omega L_c)} \qquad (17)$$

$$A_v = \frac{-r_m(1+jf/f_1)R_L(1+jf/f_4)}{(R_L+r_g)(1+jf/f_3)R_c(1+jf/f_5)} \qquad (18)$$

$$A_p = Re \frac{r_m^2 (1+(f/f_1)^2)\ R_L (1+jf/f_4)}{(R_L+r_g)^2\ (1+(f/f_3)^2)\ R_c (1+jf/f_5)} \qquad (19)$$

If no bias currents are supplied, then $r_m = r_g = 0$ and although each of the above gains is modified, amplification is still possible due to the transformer action between the input and output of the cryotron. For example, Equation(17) is changed to

$$A_v = \frac{-j\omega M\ (R_L + j\omega L_L)}{(R_L + j\omega(L_g+L_L))(R_c + j\omega L_c)} \qquad (20)$$

Similarly, if for proper bias conditions operation takes place at frequencies where $\omega M > r_m$ and $\omega(L_g+L_L) > (R_L+r_g)$, then the frequency-dependent terms will override the resistances. However, the resistances control the operation of the cryotron.

The wire-wound cryotron is thus essentially a low-frequency device, whose upper frequency limit is determined by the smallest of the break frequencies f_1, f_2, f_3, f_4 or f_5. Operation above this frequency results in amplification that is not controllable by the device.

For low-frequency operation Equations(16),(18) and (19) simplify to

$$A_i = \frac{-r_m}{r_g + R_L} \qquad (21)$$

$$A_v = \frac{-r_m\ R_L}{R_c (r_g + R_L)} \qquad (22)$$

$$A_p = \frac{r_m^2\ R_L}{R_c (r_g + R_L)^2} \qquad (23)$$

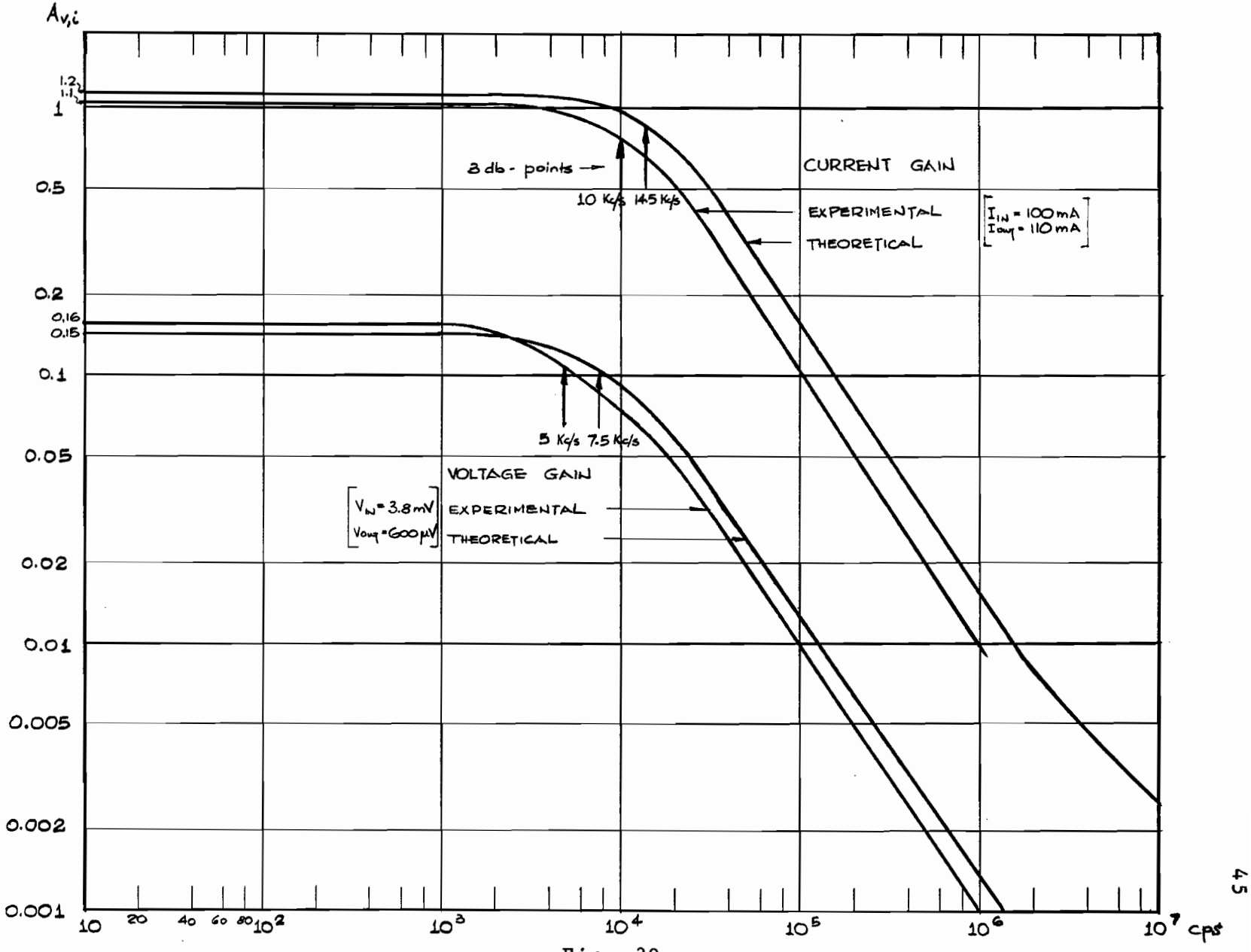

Fig. 39

Theoretical and Experimental Current and Voltage Gain Curves

and for a superconductive control winding $R_c=0$, so that the voltage and power gains become infinite, whereas for a superconductive load (cascaded cryotrons) A_v and A_p become zero and A_i a maximum. Because of the low impedances of the cryotron, any coupling and matching networks connecting these impedances to normal impedances outside the cryostat will introduce losses and the overall gains will not be infinite.

In order to theoretically predict the current- and voltage gain curves, Equations(16) and (18) were plotted in Fig.39 for the cryotron whose characteristic and transition curves are shown in Figs.29,30,31. For the calculation of the theoretical gain curves the following parameters were required.

R_c = 32 mΩ (measured)
L_c = 1.1 μh (measured)
r_g = 7 mΩ (from Fig.31)
L_g = 0.03 μh (measured)
R_L = 4 mΩ (measured)
L_L = 0.09 μh (measured)
r_m = 13 mΩ (from Fig.30)
M = 0.002 μh (estimated)

M was approximated by assuming a coefficient of coupling of one percent and the load was a 10cm-long, 40 gauge copper wire. From the parameter values the break frequencies that appear in the gain equations are calculated to be

f_1=6Mc/s, f_2=37 Kc/s, f_3=14.5 Kc/s, f_4=7 Kc/s, f_5=4.7 Kc/s.

The break frequency of the current gain curve is f_3, due to the gate and load inductances and resistances with the load impedance parameters being the dominant ones. Break frequency f_5, determined by the control winding, sets the 3-db-point for the voltage gain curve. Both curves start to roll off at 20db/decade, but beginning at 5 Mc/s they start to flatten, because the term containing f_1 in Equations(16) and (18) increases with frequency.

The experimental current gain curve was obtained by measuring the output voltage of the load and then dividing this value by the load impedance. The input current was held constant for these measurements. The voltage gain curve was obtained by measuring the output voltage for a constant input (control) voltage.

Both experimental curves have lower break frequencies than the predicted ones. The components that determine these frequencies are the control and load impedance. The resistance of these two components was measured in liquid helium, the inductances were measured at room temperature on a bridge, with the components removed from the experimental circuit. It is believed that the inductances are slightly different in the experimental circuit, due to the physical arrangement in the cryostat, giving rise to the discrepancy between experimental and theoretical values.

The frequencies of interest in cryotron operation are those at which the output voltage or current has not yet diminished, that is, frequencies at which the simple model corresponding to Equations(21) and (22) applies. From Equation (21)

$$A_i = \frac{-13\times10^{-3}}{(7+4)\times10^{-3}} = -1.2$$

Experimentally an output current of 110 mA was obtained for an input current of 100 mA; thus the experimental value of -1.1 compares favorably with the predicted value. From Equation(22)

$$A_v = \frac{-13 \times 4 \times 10^{-6}}{32 \times 10^{-3} \times 11 \times 10^{-3}} = -0.15$$

An output voltage of 600 μV was measured for an input of 3.8 mV resulting in an experimental gain of -0.16. The low voltage gain is due to the large control resistance and can be improved considerably by using a superconductive control.

For a superconductive control winding, voltage gains of 100 have been measured. According to Equation(22) the gain should be infinite, but because the inductance of the control is never zero, Equation(22) is only an approximation, that is, for any a-c control current there will always be a control voltage. A 100 mA a-c current was applied to the control of a cryotron with a 4 mΩ load and a 250 turn Nb control. At a frequency of 100 c/s this resulted in a control voltage of 40 μV and an output voltage of 400 μV. Below 100 c/s the output voltage remained constant while the input (control) voltage decreased, thus the voltage gain became larger than 100. But when the input voltage was smaller than 40μV, it could not be distinguished above the noise on the oscilloscope trace, and no numbers can be quoted for the gain.

7. Factors to be considered in the Design of Wire-Wound Cryotrons

The construction of a cryotron for a particular application involves a manipulation of various parameters, the first of which to be decided upon is the operating temperature. This determines the critical magnetic field of the gate. A number for the turns per unit length for the control is then assumed and this parameter in conjunction with an assumed control current determines the magnetic field that could be generated. Equation (24) gives the approximate magnetic field, in oersteds, for a coil of N turns per length L (cm) carrying I amperes.

$$H = \frac{4\pi}{10} \frac{NI}{L} \qquad (24)$$

Thus the temperature and approximate H_c are determined and frequently there is a choice of a few metals or alloys that fit these requirements and the one best suited as to workability and normal resistivity is selected for the gate.

Next, the type of control wire is selected with an H_c much larger than that of the gate. Niobium and lead are two typical control wires. The size of the wire is determined by the number of turns per unit length necessary to generate the required magnetic field for a suitable control current. If only one size of wire is available, it is wound to give the desired turns per unit length.

For a particular output power the parameter that need be considered is the normal gate resistance at the operating temperature. If different resistivity materials are available, the most suitable is chosen; if only one type fits the previously established temperature and magnetic field requirements, then the diameter of the gate is chosen to give the correct resistance.

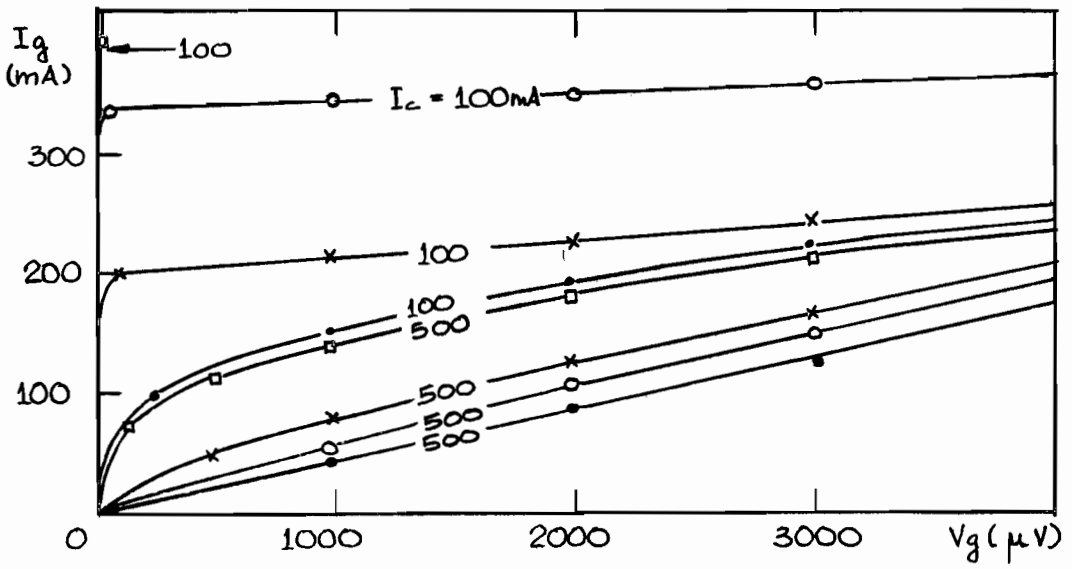

Fig. 40(a)

Characteristic Curves

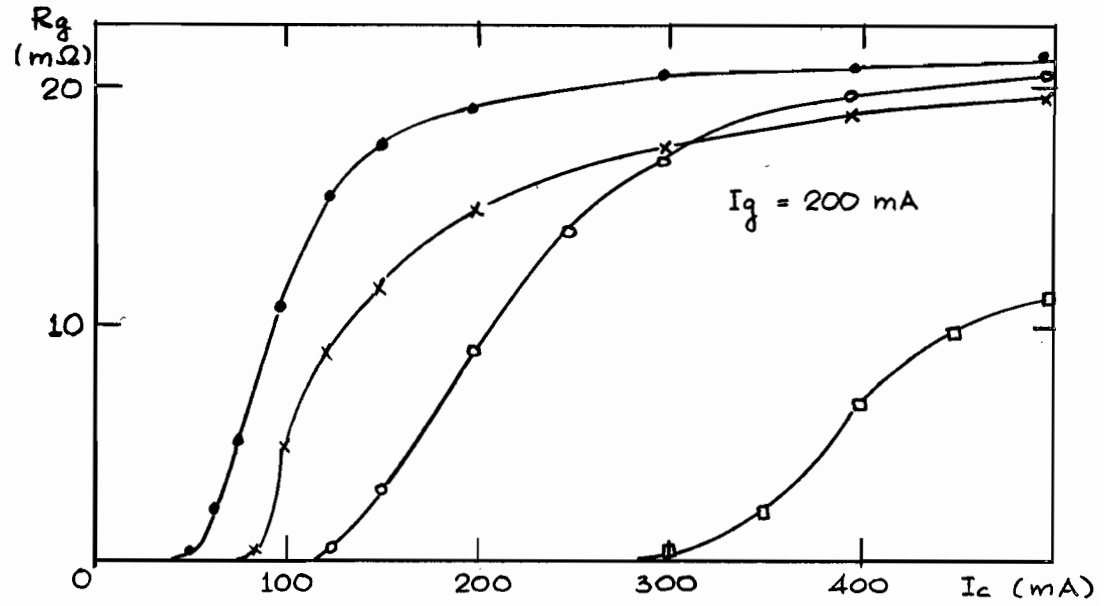

Fig. 40(b)

Resistance Transition Curves

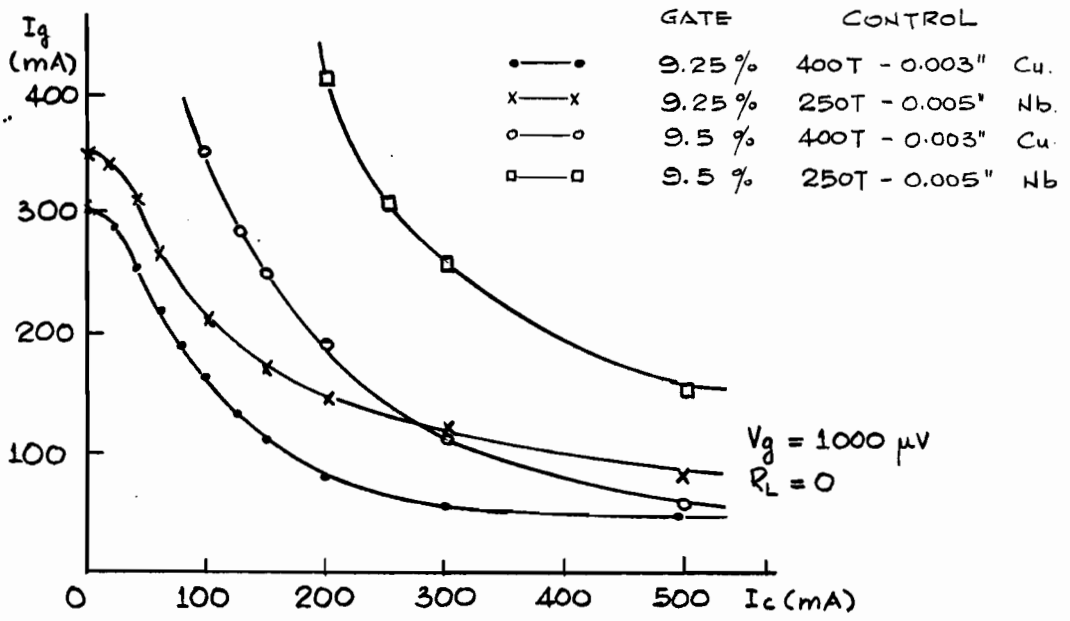

Fig. 41
Current Transfer Curves

A very convenient gate material is the lead-indium alloy, since by a variation of the percentages of the constituents a large range of critical fields is available. It is an alloy that is easily handled and extruded into various diameters.

As an illustration, a comparison was made between four cryotrons. The gate was either a 9.25 or a 9.5 atomic percent lead-in-indium alloy, 0.013 inch diameter, and the control was either of 400-turns 0.003 inch diameter copper wire, or 250-turns 0.005 inch diameter niobium wire. The number of turns was chosen so that the length of the control was equal in both cases.

The resulting characteristic, resistance transition and current transfer curves are shown in Figs.40(a), 40(b), 41. The current transfer curves yield the most obvious information regarding operation of the cryotrons. Beyond a control current of 200 mA, the curves become very flat and

operation is not desirable in this region for the 9.25% alloy, and the input signal must be in the range below 200 mA. For the 9.5% alloy, the cryotron with the 250-turn control still has a slope suitable for operation of the cryotron at a control current of 500 mA, and consequently a much larger input signal can be handled. With the higher input capability comes the disadvantage that the quiescent point is located at larger control and gate currents, resulting in more quiescent power dissipation.

Extremely large power devices can be built by a correct choice of the various parameters. Buchhold (28) built a cryotron for switching purposes that could handle up to 500 amperes. The gate was bifilarly wound of a niobium tape, surrounded by a niobium-zirconium alloy control.

8. Hysteresis

Hysteresis in the N-S transition is observed only when large gate currents are involved. On the voltage transition curves in Fig.42(a) the curves for increasing control current are shown and smooth transitions are observed for small gate currents. As I_g becomes equal to 250 mA or larger, the transitions take place in discontinuous jumps, which become more pronounced with an increase in gate current. Upon reducing the control current the transition curves follow different paths to return the gate to the superconductive state.

Fig.42(b) shows these two paths for a 300 mA gate current. Quite definitely there is a hysteresis loop traced and distinct discontinuities are clearly seen.* These discontinuities are not due to a discrete current variation, for they occur also if the change in current is continuous, as shown in Fig.42(c) which is the lower loop of Fig.42(b). Individual steps are very distinct and are reproduced for each traversal of the loop.

The loop was obtained by starting at point A, increasing the control current to trace A-D-B and then decreasing I_c gave B-C. From this point I_c was again increased to trace C-D-B and reducing the control current to zero resulted in B-C-A. The minor loop C-D-B-C was superimposed on the major loop A-B-A.

The abrupt jumps and hysteresis are both observed on the characteristic curves as well. Fig.43(a) shows the characteristic curves for increasing gate current and again

* The dot effect of the curves is due to the control current variation, determined by the output voltage of a power supply which is varied by a wire-wound potentiometer. As the wiper makes contact with adjacent turns, the output voltage, and consequently the control current, changes in small discrete steps.

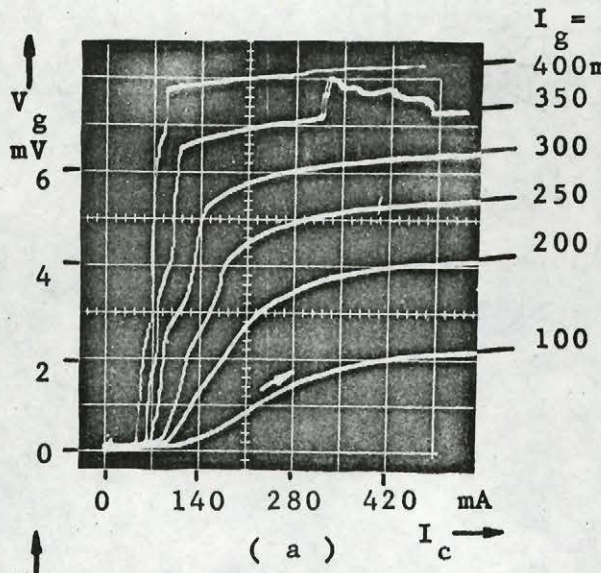

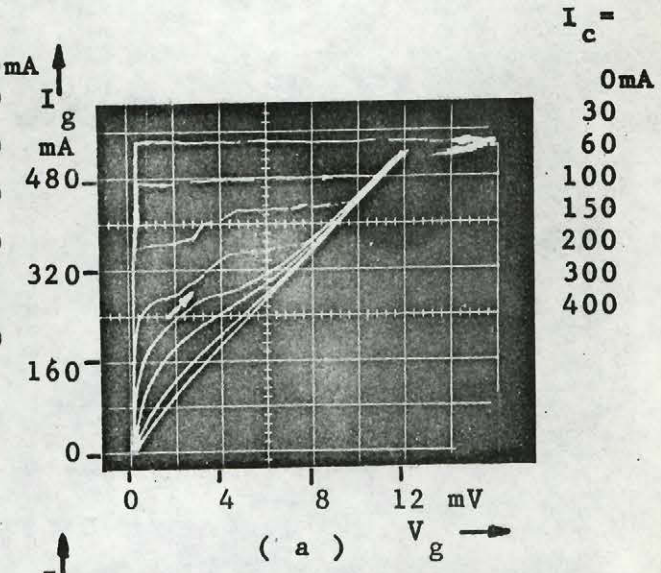

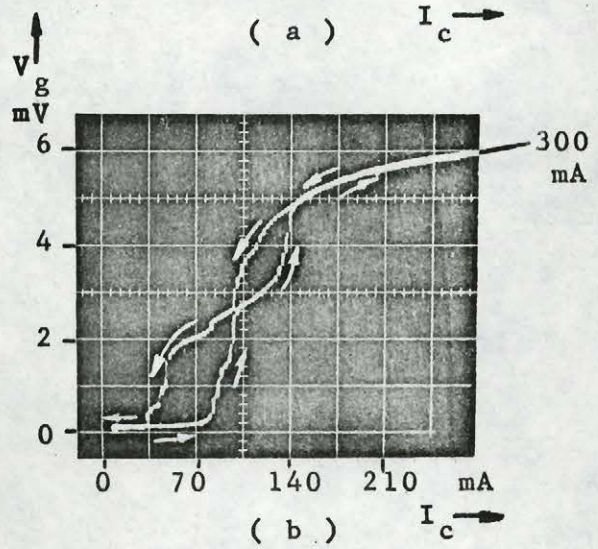

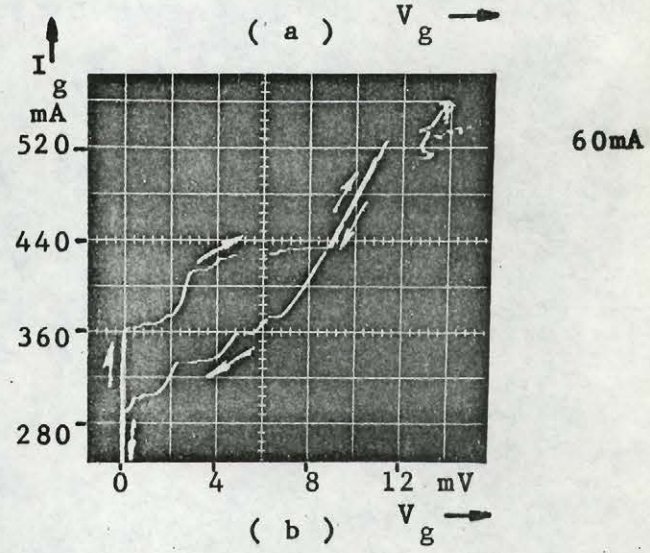

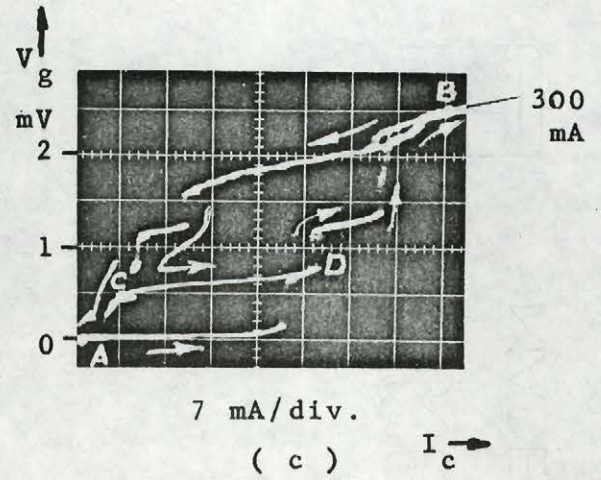

Fig. 42

Voltage Transition Curves
showing Hysteresis

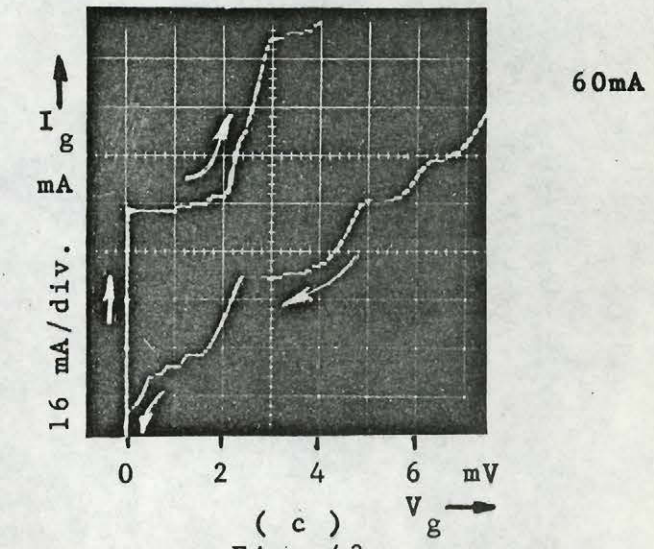

Fig. 43

Characteristic Curves
showing Hysteresis

the abrupt behavior occurs for large values of gate current. Curves of increasing and decreasing gate currents show no hysteresis for large control currents, because under these conditions the gate is mainly in the normal state. For small I_c and correspondingly large I_g, the forward transition takes place in abrupt jumps until the normal resistance curve is reached. The curve for decreasing I_g hugs the normal resistance curve longer before returning the gate to the superconductive state discontinuously. In this process a hysteresis loop is traced, as shown in Figs.43(b) and (c). Forward direction is defined as that of increasing magnetic field due to an increase in either I_c or I_g. All curves in Figs.42 and 43 were traversed slowly by manually changing the current, each one-way traversal taking place in approximately five seconds.

Superconducting hysteresis has been observed by many researchers and basically two explanations have been given. One bases the effect upon Joule heating of the specimen, the other considers 'supercooling' and'superheating'. 'Supercooling' is the persistence of the normal phase in fields less than H_c and 'superheating' the persistence of the superconducting phase in fields greater than H_c. The temperature is constant in these definitions.

Faber (29,30,31,32) placed a single crystal rod in a longitudinal, external magnetic field larger than H_c. The field was then reduced below H_c in such a manner that no transition to the S-state took place and the specimen was in the 'supercooled' state. A current pulse applied to a small coil surrounding the rod over a narrow region opposed the field. The sudden decrease in the field in this region of the rod broke down the 'supercooling' and an S-nucleus began to grow. By placing other coils along the rod the speed of propagation of this superconductive growth could be measured.

The field below which no 'supercooling' can exist is directly proportional to the imperfections in the specimen, as these lessen the degree of 'supercooling' by acting as nucleation sites. Faber concluded that the S-domains grow along the surface of the rod, but very slowly into the interior, their growth being principally governed by the N-S interphase surface energy and by eddy currents induced by the moving S-domains as they expel magnetic flux.

Similarly 'superheating' was observed when applying a field larger than H_c and still retaining the sample in the S-state. Eventually N-domains would form and then grow, again determined by the impurities acting as nucleation sites. The degree of measured 'superheating' was less than that of 'supercooling'. Meissner and Doll (33,34) measured the voltage along a tin wire for increasing and decreasing currents and obtained reproducable hysteresis loops. The voltage actually changed in many small jumps over portions of the curve, and for increasing currents these jumps were smaller than for the decreasing case. This was thought to be due to 'supercooling' and 'superheating' confirming Faber's results, since for increasing currents smaller jumps occurred ('superheating') than for decreasing currents.

Bremer and Newhouse (35) attributed the hysteresis phenomenon to Joule heating when they investigated the behavior of thin films. In the resistance transition curve they found that once the specimen was in the normal state, enough Joule heat was generated making it impossible for the helium to conduct this heat away from the film fast enough. The magnetic field had to be reduced below H_c before the change to the S-state occurred. The transition was always discontinuous and corresponded to a spontaneous growth and collapse of a resistive nucleus by thermal propagation. When the magnetic field was applied by a pulsed current through the specimen no hysteresis loops were observed.

A temperature difference across the metal-liquid helium interface is possible, because the transport of energy in helium takes place by phonons and in the metal by phonons and electrons. Because the density and velocity of sound are very much less in helium than those in a solid, an acoustic mismatch occurs at the interface giving rise to a thermal resistance, which in turn restricts the heat flow, as shown by Kapitza (36).

In this work the mode of generation and the direction of the magnetic field lies between two extremes, a circular field due to the gate current and a longitudinal field due to the control current. It is believed that the formation of domains is influenced significantly by the type of field encountered.

Consider the case of no external field, but a gate current flowing in a thin surface layer generating a magnetic field slightly less than H_c. The gate will be in the S-state as shown in Fig.44(a). As a result of a small current increase

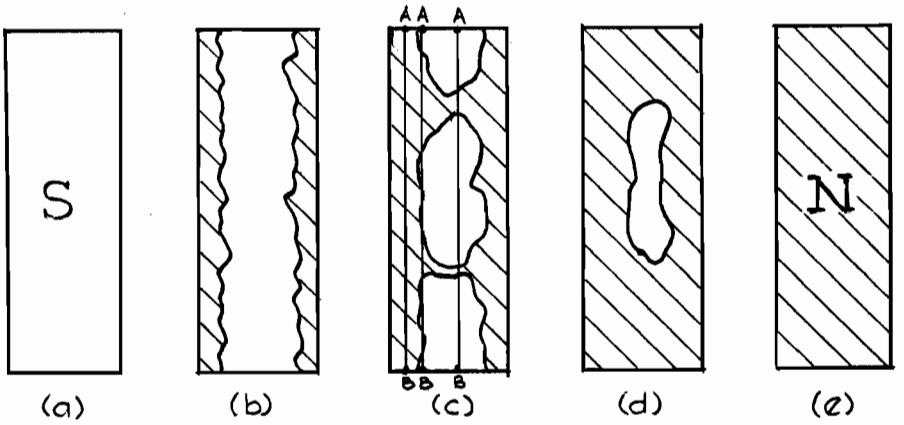

Fig. 44
S-N Transition
due to a Self-Magnetic Field

the field becomes H_c and at certain irregularities on the surface nucleation of N-domains will take place. These domains will grow along the surface and subsequently into the interior forming an approximately circular normal section as in Fig.44(b). This is an unstable situation, however, for now the current density will be higher than before, because the diameter of the S-region is reduced, and at the N-S boundary the field will be larger than H_c. Consequently, the current will distribute itself in such a manner that a portion will flow through the N-region to maintain H_c on the N-S boundary. A potential difference will result along the wire, but this is only possible if the interior goes into the intermediate state, as in Fig.44(c), so that, although the resistance is not equal between equal gate length increments, the current distribution will be such that along any path A-B the voltage will be equal. Current densities are bound to be quite high through the normal bridges resulting in some Joule heating.

The physical arrangement of the domains in Fig.44(c) is in a quasi-stable state and a small current increase can cause the collapse of large S-domains as a result of a combination of expansion of the outer N-region, formation of new bridges and possibly some Joule heating that will cause local reductions in H_c. It was observed that frequently the S-to-N transition was a very abrupt one taking place in one or two large steps. This gives reason to believe that for increasing currents the intermediate state consists of a few large domains, that is, once N-domains nucleate they either grow spontaneously throughout the entire wire, or they terminate their propagation when they enclose a few large S-domains (Fig.44(d)). A further increase in current will then cause a sudden collapse of these latter domains (Fig.44(e)).

The N-to-S transition always occurred in more steps than the S-to-N. In this case the gate starts in the N-state and upon a reduction in current, nucleation of S-domains

proceeds from the interior of the wire. It is believed that it is more difficult to nucleate an S-domain than an N-domain and this accounts for the property of the gate to remain in the N-state for smaller values of decreasing magnetic field than is necessary to produce the first trace of resistance in the S-state. Thus a hysteresis loop results.

Once an S-domain is nucleated it tends to expand gradually, as shown by a gradual reduction in resistance on the curves of decreasing I_g in Fig.45. At a certain value of current there is then a sudden resistance reduction after which the decrease is gradual again. The sudden reduction is believed to be the elimination of a normal bridge by the merging of two S-domains.

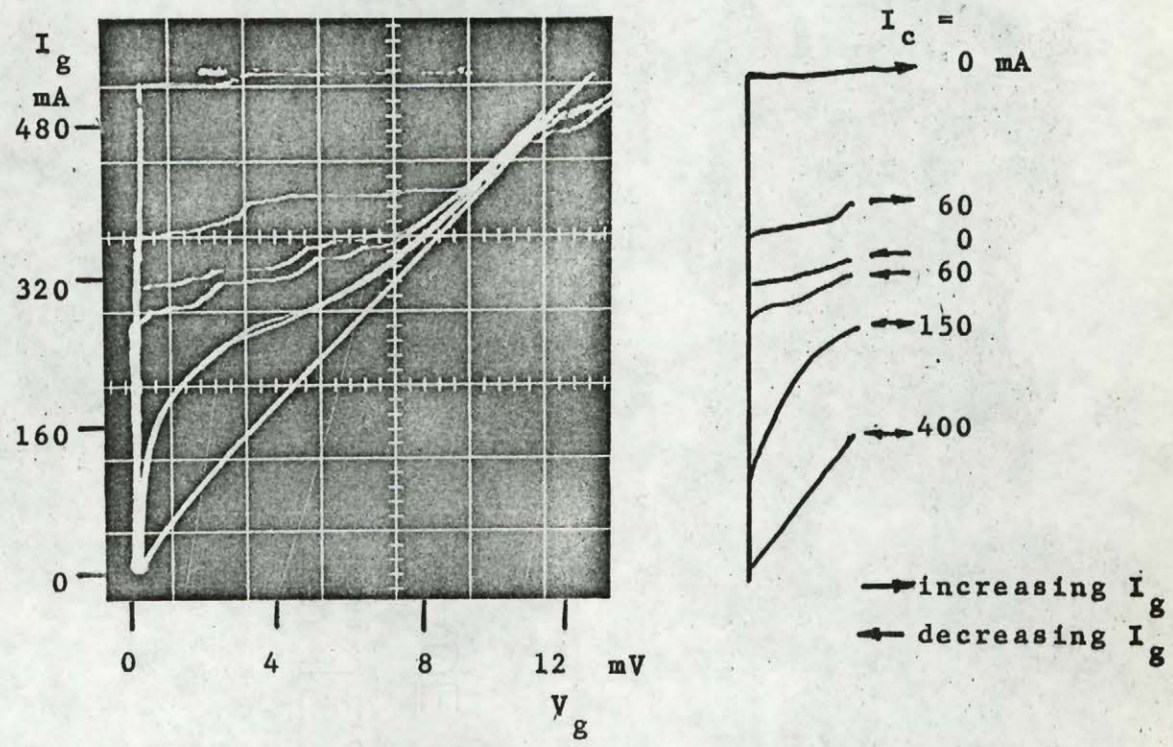

Fig. 45
Characteristic Curves
showing Hysteresis

Joule heating in the transitions is believed to be of secondary importance for the following reason. If it were the major cause then for an S-to-N transition a one-step transition would be expected, because once the first trace of resistance is restored, Joule heating would start. It would cause more of the S-region to become normal, thus generating more heat. An avalanche process of this type could only terminate with the entire wire in the normal state. But it was observed experimentally that the transitions frequently took place in several steps and the gate could even be held at some point in the intermediate state. Although it is not ruled out that this type of heating has an effect on the transition, it is believed to be of secondary importance.

The case of an external, longitudinal field,without a self-field, could not be investigated since one of the requirements of the measuring technique was a gate current. Cases of low gate current were observed and the S-to-N and N-to-S transitions were always continuous within the sensitivity of the measuring equipment. The curves for the two types of transitions coincided, that is, no discrete jumps, nor hysteresis loops were observed.

Since in this case the external field is dominant, nucleations of N-domains in S-surroundings or vice versa are believed to take place with equal ease as shown by the coincident curves. Now it is possible that either very many domains nucleate and as they grow and merge no visible discontinuities occur in the voltage along the gate, or that fewer domains form and then expand very gradually.

It is believed that the types of domains that form and the ease with which they subsequently propagate, is predominantly determined by the type of magnetic field. In the self-field case large domain motion and local H_c reduction due to Joule heat give rise to a cumulative effect, which is not observed in the case of small gate currents. To further

investigate the effect of heat, some measurements were made with the equipment immersed in helium II whose thermal conductivity is very much higher than that of helium I. Again large hysteresis loops were observed for large gate currents which tends to minimize the effect of Joule heat. However, this heating cannot be ruled out, because the interior of the gate could be at a higher temperature than the bath even in helium II, since a thermal resistance exists across the metal-helium interface.

In all cases of experimentally observed hysteresis, the area of the hysteresis loop is very dependent upon the magnitude of the gate current. It is believed that hysteresis finds its origin mainly in the difficulty of nucleating S-domains in a normally-resistive wire when the self-field is dominant.

9. Noise

Partition, shot and generation-recombination noise should be absent in the cryotron, because there are no grids, no heated surfaces and only one type of carrier. Thermal or Johnson noise will be small because the device is operated at approximately 4°K and the resistances are very small. Current noise, defined as the noise due to fluctuations in the resistivity of a resistive element, is present since the resistance of the gate changes during cryotron operation. But these changes in resistance take place as a result of domain size variation, resulting in Barkhausen noise (38) which was discovered when discrete jumps of magnetic domains were observed during the magnetization of iron.

To detect the movement of domains, use was made of the diamagnetic properties of an S-domain. As a region becomes superconductive, its magnetic flux is expelled inducing a voltage in a search coil wound tightly around the gate. The search coil consisted of 400 turns, 40 gauge wire with half the turns wound in opposition to the other half. This was done to eliminate any pickup from fluctuations in the external magnetic field.

The external field was generated by either winding a control coil around the search coil, or by an external solenoid into which the gate with search coil was inserted. Two solenoids, 50mm long and 7.5mm inside diameter, wound of 10,000 turns copper and niobium wire were used. By changing the external field,transition curves were traversed and voltages were induced in the search coil.

After amplifying the search coil induced voltage, it was measured on a recorder and galvanometer. But only those noise voltages induced by steplike discontinuities on the transition curves were observed. On traversing the 'smooth' curves no induced voltages were observed, indicating

that if a 'smooth' transition really took place by small discrete steps, these induced voltages so small that they could not be measured due to the background noise of the measuring equipment.

Van Oijen and Druyvesteyn(39) have observed noise voltages over certain ranges of transition curves. However, they did not show the relevant transiton curves and it is not clear what type of transitions were involved in their experiments.

When the noise measurements were made it was observed that even for constant gate current and external magnetic field, fluctuations in the gate resistance were observed as long as the gate was biased in the intermediate state. These fluctuations occurred whether the external magnetic field was supplied by a control coil wound around the gate, by a solenoid or by a permanent magnet outside the cryostat. Sometimes these gate resistance changes were of a periodic relaxation manner, at other times they were very irregular (see Figs.46 and 47). Search coil induced voltages showed that doamin motion was involved, and the resistance changes are thus due to domain expansion and contraction.

It appears that the fluctuations are thermally induced, because the periodic oscillations disappeared when the helium bath temperature was reduced below the lambda point.They also disappeared when a heating coil was installed below the apparatus in the helium, because the bubbling helium created by the heater destroyed any possible thermal stratification.

No fluctuations were observed when the cryotron was placed next to a ground plane, possibly because the heat conductivity of lead is very much greater than that of helium (approx. 20 watts/cm $^{\circ}$K for lead, 2.7×10^{-4} watts/cm $^{\circ}$K for helium, both at 4°K), resulting in a more uniform temperature along the vertically held cryotron. Almost no fluctuations were observed for a horizontally held cryotron with no ground plane.

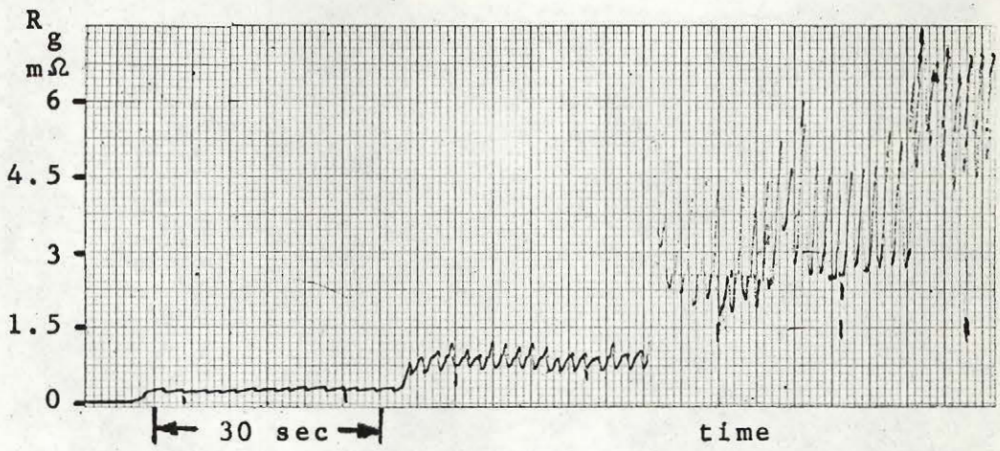

Fig. 46

Periodic Resistance Fluctuations
(I_g=150 mA, I_c is constant for each level)

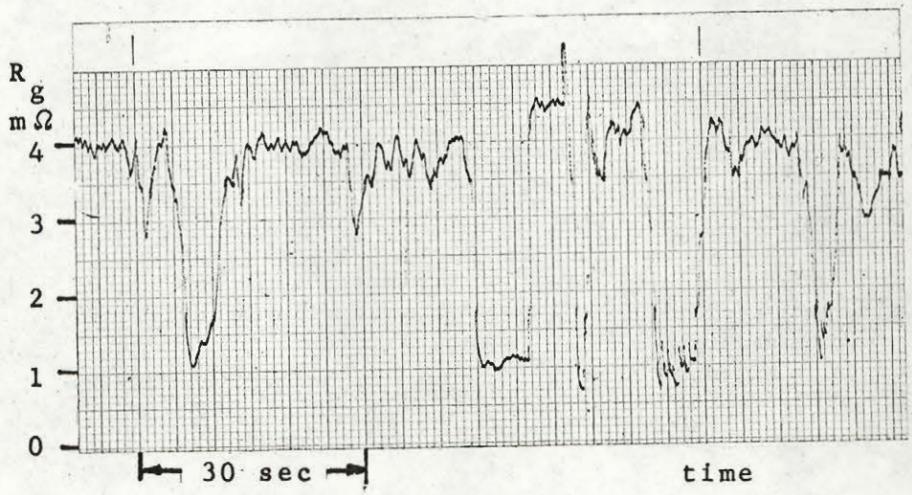

Fig. 47

Aperiodic Resistance Fluctuations
(I_g=225 mA, I_c= 30 mA)

Helium evaporates constantly in the cryostat as seen by bubbles rising in the liquid even when no power is dissipated in the cryotron. A thermal stratification is thus possible which is agitated and can cause small temperature changes along the gate. These small changes will appreciably change H_c, because the cryotron operates on the steep portion of the H_c vs. T curve (Fig.12) near the transition temperature. For a constant magnetic bias field, fluctuations will take place in the gate resistance.

To determine the effect of small temperature changes, an open tube water manometer was attached to an opening provided for this purpose in the head plate. Opening or closing the filling hole in the head plate by a rubber stopper varied the pressure in the cryostat from atmospheric to as much as 30 cm water (approx. 2 cm mercury) above atmospheric pressure. This is equivalent to a temperature rise of 0.03°K and for this change the gate resistance varied between mean values of two and ten milli-ohms (normal gate resistance = 20 mΩ). Superimposed on these mean values, at each pressure level, were the type of fluctuations discussed above.

The fluctuations were therefore not the result of pressure variations, because they were observed when the pressure was at atmospheric pressure or had stabilized at some higher value. It was considered stabilized when no change in the water level was noticed. Rather, the resistance fluctuations are believed to be the result of temperature variations within the liquid helium bath. Fig.47 shows resistance changes of about three milli-ohms which corresponds to a temperature change of less than 0.02°K, according to the experimental values above of eight milli-ohms change for a temperature variation of 0.03°K. These temperature variations of a few hundredths of a degree are likely to occur in the helium bath.

Associated with these resistance fluctuations is a Barkhausen noise and for low-noise operation the cryotron should be placed on a ground plane. Operation should also take place along the 'smooth' transition curves, because biasing in the unstable region is undesirable not only from the instability condition, but also because this is the region of large noise voltages.

10. Conclusions

The two main parts of this work are the amplifying and frequency characteristics of the wire-wound cryotron, and the intermediate state properties of the gate, for it is in the intermediate state that the device operates as an amplifier.

The results of the first part show that the wire-wound cryotron is inherently a low-frequency device, because at liquid helium temperatures any resistances of interest are small, so that inductances which are negligible at room temperature become extremely important. The high-frequency response for current amplification is mainly limited by the break frequency of the load impedance, and the control circuit determines the break frequency of the voltage gain curve. Current gains above unity were observed and voltage gains of 100 were measured for a superconducting control winding. No low-frequency limitation exists in the operation of the cryotron and application as a d-c amplifier is feasible, provided the quiescent point is stabilized by the control and gate bias currents.

In the region of large gate current operation (unstable region) resistive jumps occur on the S-to-N and N-to-S transitions, when the self-magnetic field of the gate is the dominant component of the total magnetic field. The discontinuities are the result of large, abrupt domain movements due to a self-field increase or decrease, combined with Joule heating which aids by locally reducing the critical field.

Observed hysteresis in the unstable region is believed to be due mainly to the difficulty of nucleating superconducting domains in a normally resistive wire.

Barkhausen noise, caused by domain movements, was measured in the unstable region of the cryotron operation, where the transitions between the superconductive and normal states and vice versa take place by abrupt discontinuities. Along the 'smooth' transitions of small gate currents no induced noise voltages were measured, indicating that if Barkhausen noise did exist it was too small to be measurable with the experimental equipment.

Thus for low noise and stable operation of the cryotron as an amplifier, the device should be biased in the 'active region' (defined in chapter 6). The cryotron should also be placed on a ground plane for the gate resistance not to be changed by any temperature fluctuations within the helium bath.

Bibliography

1. Templeton, I.M.
   A Superconducting Reversing Switch,
   J.Sci.Instr., 32, pp.172-173, 1955

2. A Superconducting Modulator,
   J.Sci.Instr., 32, pp.314-315, 1955

3. De Vroomen, A.R., Van Baarle, C.
   A Sensitive Superconducting 'Chopper' Amplifier,
   Physica, 23, pp.785-794, 1957

4. Templeton, I.M.
   Superconductive Devices and Electrical Measurements at Low Temperatures,
   Int.Solid State Cct.Conf., Philad., pp.68-69, 1960

5. Buck, D.A.
   The Cryotron - A Superconductive Computer Component,
   Proc.IRE, 44, pp.482-493, 1956

6. IRE Standards
   IRE Standards on Superconductive Terms,
   Proc.IRE, 50, p.452, 1962

7. Parkins, G.
   A Cryotron Equivalent Circuit,
   New York University, M.S.Thesis, 1959

8. Chirlian, P.M., Marsocci, V.A.
   Controlled Superconductor as Linear Amplifier,
   IRE Trans., CP-8, pp.84-88, 1961

9. On the Linear Aspects of Cryotrons,
   Proc.IRE, 49, p.1326, 1961

10. Optimization of the Dynamic Parameters of the Controlled Superconductor,
    IRE Trans., CP-9, pp.74-77, 1962

11. Operational Amplifiers using Controlled Superconductors,
    IRE Trans., EC-11, pp.6-9, 1962

12. A Cryotron Linear Amplifier,
    IEEE Trans., CP-10, pp.144-146, 1963

13. Valentir, S., Haberstroh, A.
Ueber das System Indium-Blei,
(On the System Indium-Lead),
Z.Phys., 110, pp.727-741, 1938

14. Jones, H.
Transition Temperatures of Superconducting Alloys,
Nature, 142, p.611, 1938

15. Gygax, S.
Ein Supraleitender Gleichspannungsverstaerker fuer
Helium Temperaturen,
(A Superconductive D-C Voltage Amplifier for
Helium Temperatures)
Z.Angew.Math.Phys., 12, pp.289-297, 1961

16. Richards, N.D.
The Cryotron as a Small Signal HF Amplifier,
Int.Solid State Cct.Conf., Philad., pp.64-65, 1962

17. Shoenberg, D.
Superconductivity,
Cambridge University Press, Ch.3 and 4, 1952

18. Meshkovskii, A.G., Shal'nikoff, A.I.
Structure of Superconductors in the Intermediate State,
J.Phys.USSR, 11, p.1, 1947

19. Schawlow, A.L.
Structure of the Intermediate State in Superconductors,
Phys.Rev., 101, pp.573-579, 1956

20. Schawlow, A.L., Devlin, G.E.
Intermediate State of Superconductors,
Influence of Crystal Structure,
Phys.Rev., 110, pp.1011-1016, 1958

21. Schawlow, A.L., Devlin, G.E., Hulm, J.K.
Intermediate State of Hard Superconductors,
Phys.Rev., 116, pp.626-627, 1959

22. Baloshova, B.M., Sharvin, Yu.V.
Structure of the Intermediate State of Superconductors,
JETP USSR, 4, pp.54-59, 1957

23. Faber, T.E.
The Intermediate State in Superconducting Plates,
Proc.Roy.Soc., A248, pp.460-481, 1958

24. Shubnikov, L., Nakhutin, I.
Electrical Conductivity of a Supraconducting Sphere in the Intermediate State,
Nature, 139, pp.589-590, 1937

25. Shal'nikoff, A.I.
Concerning the Reality of the Nonstationary Model of the Intermediate State,
JETP USSR, 6, pp.827-828, 1958

26. McFee, R.
Optimum Input Leads for Cryogenic Apparatus,
Rev.Sci.Instr., 30, pp.98-102, 1959

27. Sobol, H., McNichol, J.J.
Evaporation of Helium I due to Current Carrying Leads,
Rev.Sci.Instr., 33, pp.473-477, 1962

28. Buchhold, T.A.
Cryogenic Flux Pump Switches High Currents,
Electronics, 37, no.12, pp.61-63, 1964

29. Faber, T.E.
The Phase Transition in Superconductors,
I Nucleation,
Proc.Roy.Soc., A214, pp.392-412, 1952

30. II Phase Propagation Above the Critical Field,
Proc.Roy.Soc., A219, pp.75-88, 1953

31. III Phase Propagation Below the Critical Field,
Proc.Roy.Soc., A223, pp.174-194, 1954

32. The Supercooling Effect in Superconductors close to the Transition Temperature,
Proc.Roy.Soc., A241, pp.531-546, 1957

33. Meissner, W., Doll, R.
Ueber die Entstehung von Hysteresisschleifen der Widerstandskurven im Uebergangsgebiet zur Supraleitung,
(On the Formation of Hysteresisloops on the Resistance Curves in the Transition Region of Superconductivity),
Z.Phys., 154, pp.524-533, 1959

34. Die Eigenschaften der Widerstands-Hysteresisschleifen im Uebergangsgebiet zur Supraleitung, (Properties of Resistance-Hysteresisloops in the Transition Region of Superconductivity), Z.Phys., 156, pp.488-502, 1959

35. Bremer, J.W., Newhouse, V.L.
Current Transition in Superconductive Thin Films, Phys.Rev., 116, pp.309-313, 1959

36. Little, W.A.
The Kapitza Resistance of Metals in the Normal and Superconducting States, IBM J.Res.Dev., 6, pp.31-33, 1962

37. DeSorbo, W., Healy, W.A.
The Intermediate State of Some Superconductors, General Electric Res. Rep. No.61-RL-2743M, 1961

38. Barkhausen,H.
Zwei mit Hilfe der Neuen Verstaerker entdeckte Erscheinungen, (Two Phenomena discovered with the Aid of New Amplifiers), Phys.Zeit., 20, pp.401-403, 1919

39. Van Oijen, D.J., Druyvesteyn, W.F.
Analogon of Barkhausen Noise Observed in a Superconductor, Phys.Lett., 6, pp.30-31, 1963